REPORT OF INVESTIGATIONS/1991



# Flywheel-Powered Shuttle Car

By John R. Bartels, William D. Mayercheck,
and Jon A. Hummer

UNITED STATES DEPARTMENT OF THE INTERIOR

BUREAU OF MINES

**Mission:** As the Nation's principal conservation agency, the Department of the Interior has responsibility for most of our nationally-owned public lands and natural and cultural resources. This includes fostering wise use of our land and water resources, protecting our fish and wildlife, preserving the environmental and cultural values of our national parks and historical places, and providing for the enjoyment of life through outdoor recreation. The Department assesses our energy and mineral resources and works to assure that their development is in the best interests of all our people. The Department also promotes the goals of the Take Pride in America campaign by encouraging stewardship and citizen responsibility for the public lands and promoting citizen participation in their care. The Department also has a major responsibility for American Indian reservation communities and for people who live in Island Territories under U.S. Administration.

Report of Investigations 9329

# Flywheel-Powered Shuttle Car

By John R. Bartels, William D. Mayercheck,
and Jon A. Hummer

UNITED STATES DEPARTMENT OF THE INTERIOR
Manuel Lujan, Jr., Secretary

BUREAU OF MINES
T S Ary, Director

**Library of Congress Cataloging in Publication Data:**

**Bartels, John R.**

Flywheel-powered shuttle car / by John R. Bartels, William D. Mayercheck, and Jon A. Hummer.

p. cm. — (Report of investigations / United States Department of the Interior, Bureau of Mines; 9329)

Includes bibliographical references.

Supt. of Docs. no.: I 28.23:9329.

1. Shuttle cars (Mine haulage)—Motors. 2. Flywheels. I. Mayercheck, William D. II. Hummer, Jon A. III. Title. IV. Series: Report of investigations (United States. Bureau of Mines); 9329.

TN23.U43 [TN342] 622 s—dc20 [622'.66] 90-2346 CIP

## CONTENTS



## ILLUSTRATIONS

## ILLUSTRATIONS—continued



## TABLES

## UNIT OF MEASURE ABBREVIATIONS USED IN THIS REPORT

| | |
|---|---|
| A | ampere |
| dB | decibel |
| °F | degree Fahrenheit |
| °F/s | degree Fahrenheit per second |
| ft | foot |
| $ft^3$ | cubic foot |
| ft·lb | foot pound |
| Gal | acceleration due to gravity |
| gal | gallon |
| gpm | gallon per minute |
| h | hour |
| hp | horsepower |
| Hz | hertz |
| in | inch |
| in/s | inch per second |
| J | joule |
| kW | kilowatt |
| kW·h | kilowatt hour |
| L/min | liter per minute |
| lb | pound |
| lb/st | pound per short ton |
| $\mu$F | microfarad |
| $\mu$H | microhenry |
| min | minute |
| mph | mile per hour |
| pct | percent |
| psi | pound per square inch |
| psia | pound per square inch, absolute |
| psig | pound per square inch, gauge |
| rpm | revolution per minute |
| rpm/s | change in revolution per minute per second |
| s | second |
| st | short ton |
| V | volt |
| V ac | volt, alternating current |
| V dc | volt, direct current |
| W | watt |
| W·h | watt hour |
| W·s | watt second |

# FLYWHEEL-POWERED SHUTTLE CAR

By John R. Bartels,[1] William D. Mayercheck,[2] and Jon A. Hummer[3]

## ABSTRACT

This U.S. Bureau of Mines report describes the development, system by system evaluation, and preliminary surface testing of a flywheel-powered shuttle car (FPSC). The use of a self-contained flywheel-power source has the potential to eliminate the numerous safety and routing problems associated with tethered mobile equipment. An alternative to conventional power cable systems was developed consisting of the world's first seven-rotor stacked flywheel system capable of storing 6 kW·h of energy at 16,700 rpm. Numerous interdependent systems were necessary for successful interfacing with a conventional shuttle car. Each of these systems was evaluated and tested individually. Finally, the entire shuttle car was surface tested. The tests indicated that the flywheel energy system can function and operate a shuttle car. The economics of the system and the design of required support systems were not addressed in the project

[1]Civil engineer, Pittsburgh Research Center, U.S. Bureau of Mines, Pittsburgh, PA.
[2]Supervisory physical scientist, Pittsburgh Research Center.
[3]Electrical engineer, Schneider Services, Pittsburgh, PA.

## INTRODUCTION

The trailing cable constitutes a major drawback to shuttle car safety and productivity. To avoid tangled or damaged cables, each shuttle car must have a dedicated route. Naturally, there are only a few entries available for these routes in the mine. The cables are often a source of electrical accidents, and the tensioning system often causes injuries. Production delays are also caused by cable maintenance and handling. The FPSC has the potential to be safer and more efficient than conventional shuttle cars because of the elimination of the trailing cable. The FPSC is not restricted to using the same forward and return path, thus allowing more than two shuttle cars to operate in a section. Computer simulations have indicated that this technology would achieve a lower cost per short ton and higher rate of return than other coal haulage vehicles powered by conventional electric motors.[4]

Trailing cable restrictions can be eliminated by a self-contained power source on the shuttle car. However, the more conventional means of providing power, such as the internal combustion engine, is not permissible in some States due to the closed environment. Flywheel power is especially suited for use in hazardous areas because it eliminates the need for an electrical trailing cable.

The potential use of a FPSC permits the use of a number of such cars in a section to improve productivity and increase safety while freeing the car from restraints inherent with use of the trailing cable.

The Pennsylvania State University-U.S. Bureau of Mines (PSU-USBM) computer simulation model was then used to determine the effects of various bottom conditions and seam thicknesses on the energy requirements for the flywheel. The results of the simulation and the calculations from the mine data were reviewed, and it was determined that the flywheel design should be based on 4.5 kW·h of usable energy. This represented a balance between the high values obtained with the computer simulation of requirements in high coal with bad bottom and the low values from the actual mine tests. This power requirement was to perform a duty cycle with a tram distance of 550 ft from the face to the dump site on a ±3 pct grade with a rolling resistance of 200 lb/st.

The FPSC (fig. 1) was designed and fabricated by the Engineered Systems & Development (ESD) Corp., San Jose, CA under a Bureau contract.[5] The flywheel module chosen to meet this energy requirement and still fit within the limited space available on a standard shuttle car was a compact seven-rotor module (fig. 2). This module is capable of storing a total of 6,000 W·h of energy at 16,700 rpm with 4,500 W·h of usable energy, which permits the car to complete the duty cycle with 700 W·h of energy in reserve (fig. 3). Specifications for the flywheel-power system are detailed in table 1. Table 2 is a comparison of the FPSC with other haulage equipment in its class.

[4]General Electric Co. Evaluation of a Flywheel-Powered Shuttle Car (Dep. Energy contract ET77C01-8890), Aug. 1978, 128 pp.

[5]Christofferson, D. Flywheel-Powered Shuttle Car (contract J0333911, Engineered Systems & Development Corp.) BuMines OFR 96-86, 1986, 173 pp.; NTIS PB 87-119079.

**Figure 1.—Flywheel-powered shuttle car.**

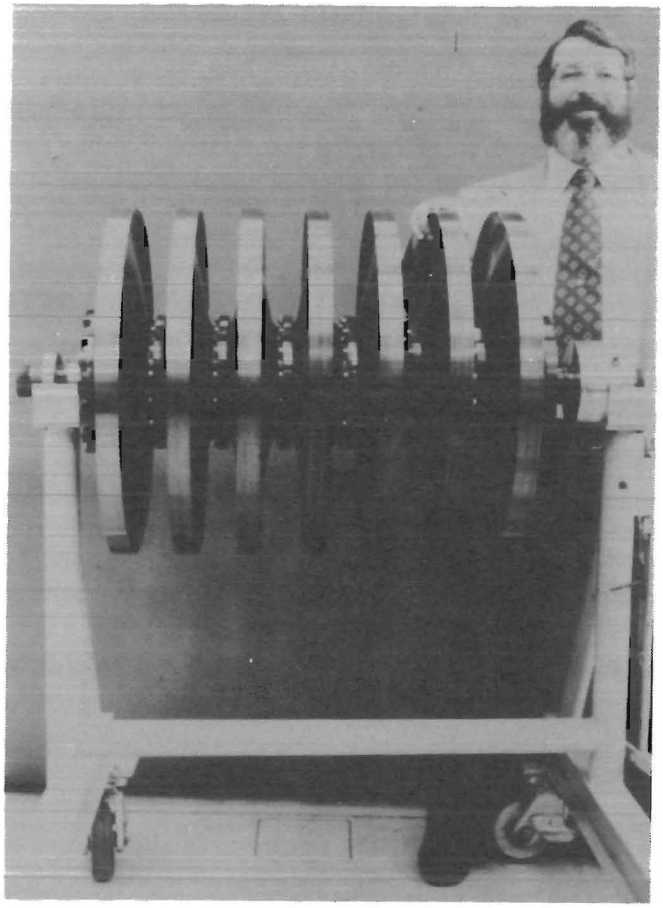

Figure 2.—Seven-rotor configuration.

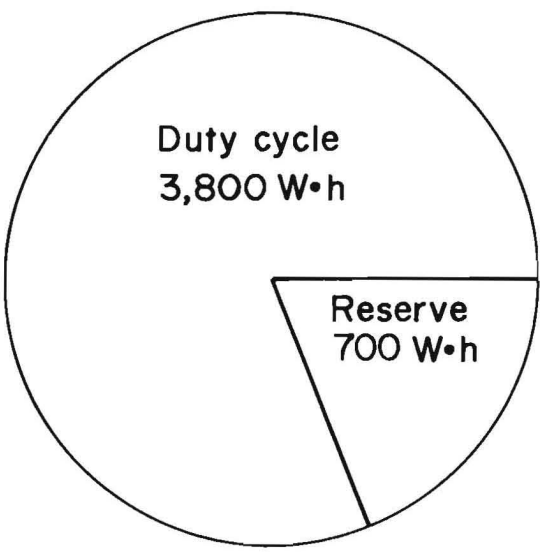


Figure 3.—Duty cycle.

Table 1.—Flywheel-powered shuttle car[1] specifications

| | | |
|---|---|---|
| Shuttle car: | | |
| Weight (empty), with flywheel drive package | lb | 30,000 |
| Length | ft | 24 |
| Height, in: | | |
| Frame | | 34.5 |
| Top of canopy | | 50 |
| Minimum working height with canopy | | 56 |
| Width | in | 112.5 |
| Conveyor: | | |
| Width | in | 56 |
| Speed | rpm | 64 |
| Capacity, ft$^3$: | | |
| Level | | 186 |
| With 6-in sideboards | | 272 |
| Maximum tram speed[2] | mph | 4.2 |
| Tires: | | |
| Size | | 10 by 15 |
| Load rating (each) | lb | 16,000 |
| Ground clearance | in | 7.5 |
| Wheel base | in | 98 |
| Boom, in: | | |
| Extension | | 41 |
| Clearance: | | |
| Up | | 35.25 |
| Down | | 10.25 |
| Turning radius, in: | | |
| Inside | | 109 |
| Outside | | 257 |
| Motor (250 V dc) rating, hp: | | |
| Traction (2) | | 15 |
| Chain conveyor | | 15 |
| Hydraulic pump | | 15 |
| Energy, kW•h: | | |
| Maximum gross storage at 16,700 rpm | | 6 |
| Net usable (16,700-12,800 rpm) | | 4.5 |
| Flywheel drive weight, excluding onboard charge system | lb | 3,250 |
| Onboard charge motor (480 V ac) rating | hp | 300 |
| Lube-cooling system rate at 230 psi | gpm | 34.6 |
| Vacuum pump pressure in flywheel housing, psia: | | |
| Minimum | | 0.2 |
| Maximum | | 0.02 |
| Power generator from flywheel rotor | V dc | 270 |
| Flywheel, in: | | |
| Rotor (7) diameter | | 23 |
| Housing: | | |
| Diameter | | 27.5 |
| Length | | 45 |
| Drive space envelope: | | |
| Width | | 28 |
| Height | | 34 |
| Length | | 76 |

[1]FMC model 6L.
[2]With silicon-controlled rectifiers.

Table 2.—Comparison of various face haulage vehicles

| Manufacturer and model | Energy, kW-h | | Total onboard hp | Payload (water level) | | Total weight empty, lb |
|---|---|---|---|---|---|---|
| | Stored | Duty cycle | | ft³ | st | |
| FMC 6L-56: | | | | | | |
| Flywheel powered | 6.0 | 3.8 | 60 | 186 | 5.1 | [1]30,000 |
| Electric trailing cable | 6.0 | 3.8 | 60 | 186 | 5.1 | 24,000 |
| FMC 6L-48 | NAp | NAp | 60 | 160 | 4.4 | 22,000 |
| Joy 18SC-13 | NAp | 3.95 | 55 | 190 | 5.2 | 26,000 |
| National Mine Service Co: | | | | | | |
| T-20 Torkar | NAp | 2.07 | 45 | 154 | 4.2 | 23,000 |
| MC36-S12[2] | NAp | NAp | 100 | 194 | 5.3 | 28,000 |
| Jeffrey 404L RAMCAR[2] | 70 | NAp | 50 | 134 | 3.6 | 27,000 |
| Kersey 16-S | 70 | NAp | 40 | 110 | 3.0 | 32,000 |

NAp Not applicable.
[1]Includes onboard 300-hp, 480-V ac charge motor and gearbox (2,750 lb total).
[2]Battery powered.

## DESCRIPTION OF FLYWHEEL-POWERED SHUTTLE CAR

The FPSC is a conventional FMC[6] model 6L shuttle car retrofitted with a flywheel-power package. The flywheel-power package is located in the area previously occupied by the cable reel. The shuttle car has a 6-st haulage capacity and a 15-st gross vehicle weight. A solid-state starter is connected to a 300-hp charging motor, charging the flywheel to 16,700 rpm. Energy for shuttle car operation is extracted from the flywheel via a 270-V dc generator. Figure 4 is a detailed illustration of the flywheel package with components.

[6]Reference to specific products does not imply endorsement by the U.S. Bureau of Mines.

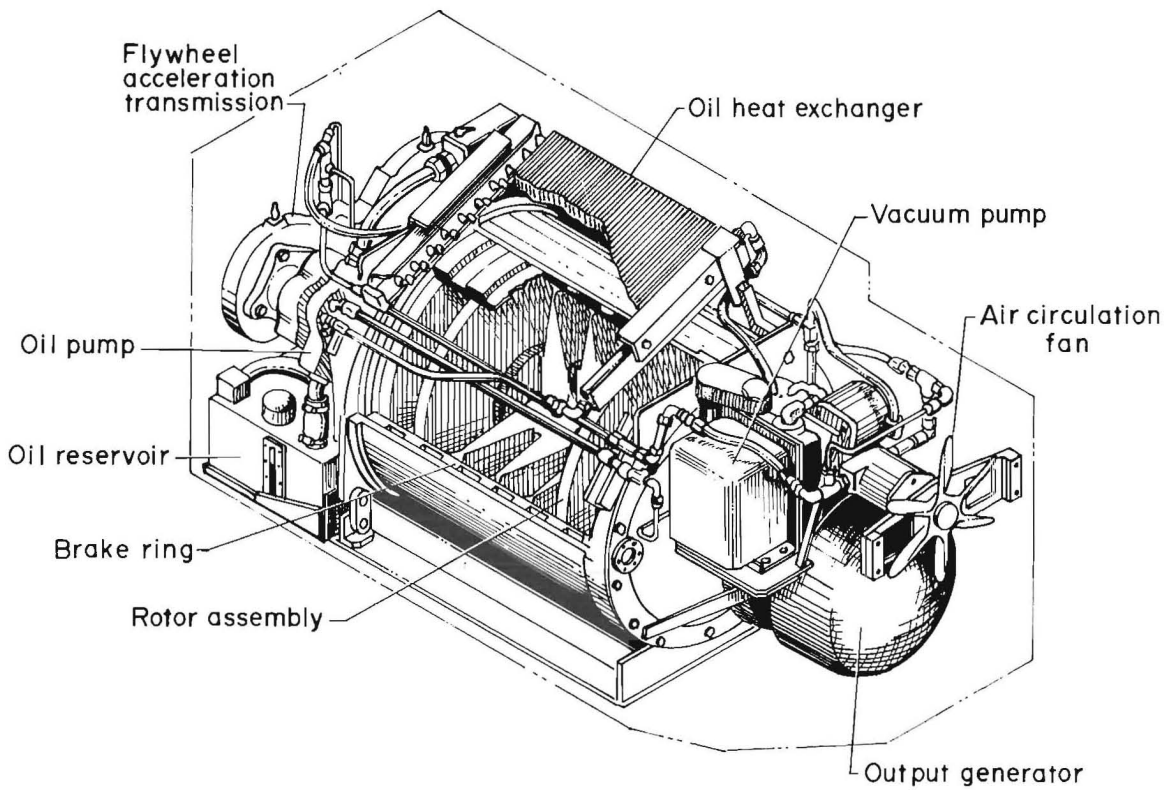


Figure 4.—Flywheel module.

## FLYWHEEL CHARGE MOTOR

Figure 5 shows the charge motor mounted on the shuttle car. The charge motor is rated at 300 hp (nominal) and is a three-phase, 460-V, 60-Hz, alternating current (ac) squirrel cage induction motor. Figure 6 defines the motor characteristics.

The mine-permissible induction motor was specified to meet the required duty cycle, i.e., spin up from 12,800 to 16,700 rpm in less than 60 s on the duty cycle once every 6 min. The specified duty cycle represents an average condition compatible with duty cycle measurements taken from in-mine measurements and computer simulation. The charge motor is critical to the successful operation of the flywheel-powered system because for mining applications a fast recharge time is required for the mine production cycle. The charge motor would not be mounted on the machine for in-mine application and is only mounted on the machine for proof of concept evaluation.

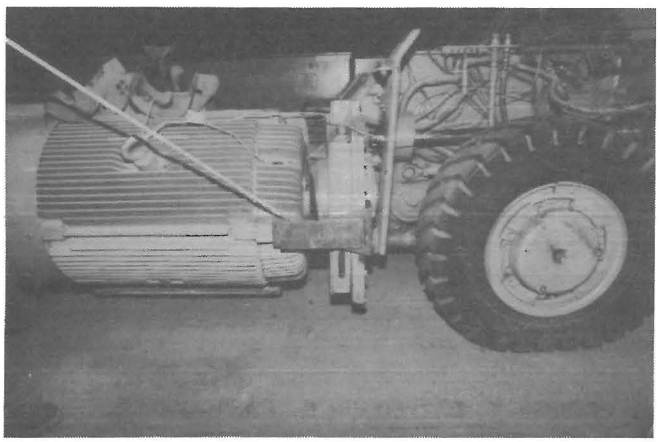

Figure 5.—Charge motor.

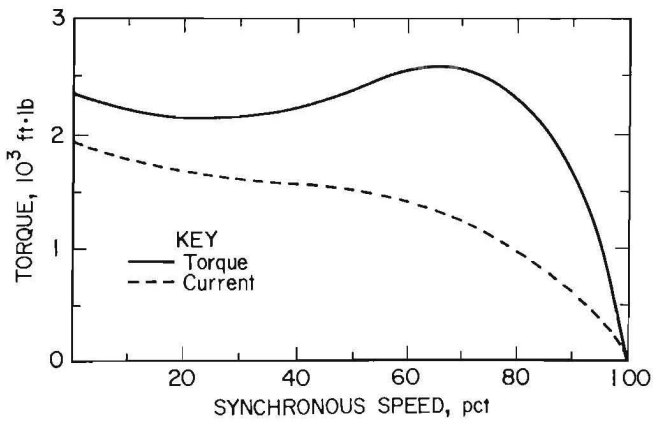


Figure 6.—Motor characteristics.

## SOLID-STATE STARTER

A solid-state starter provides soft start capability for the charge motor (class 15-30657 starter). The starter causes an altered torque-speed curve, for lower shockload and prevention of excessive charge motor heat generation. The starter allows the charge motor to more readily interface the high inertial force of spinning the flywheel up to speed from a dead stop condition.

The solid-state starter contains a number of silicon-controlled rectifiers (SCR), which switch the incoming 480-V electrical lines at synchronized intervals during the 60-Hz voltage alternations. By advancing or delaying the triggering points, more or less power can be applied to the charge motor. When charging the flywheel, it is desirable to start the motor with a minimum of voltage and to increase gradually the amount as the flywheel accelerates. Figure 7 shows the solid-state starter.

The following adjustments are available on the starter:

1. Current Limit - Determines the maximum current draw that the charge motor is permitted. The reduced current capability prevents the motor from imposing excessive output torque.
2. Current Trip - Turns off the starter and lights a red indicator when a running overload has occurred. A 40-s time delay after the start command enables the motor to come up to speed before the trip becomes active. The trip can be set between 75 and 150 pct of the motor's full-load current rating.

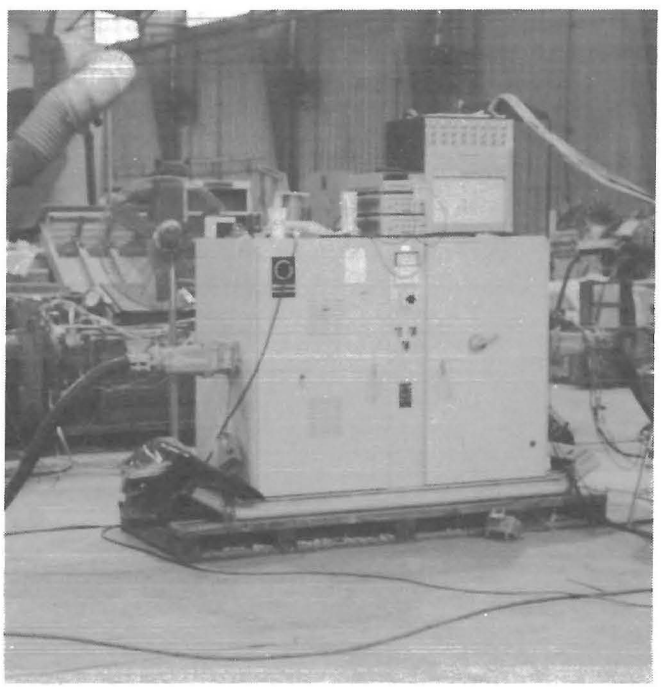

Figure 7.—Solid-state starter.

3. Ramp Time - This system selects the rate of linear voltage increase until full-line voltage is reached. A current limit override may extend the ramp time. The control is adjustable from 1 to 30 s.

4. Initial Voltage - This system sets the initial voltage to a level that enables the motor to exceed breakaway torque when it is just started. The adjustment can vary the initial voltage from 0 to 50 pct of line voltage.

## SYSTEM GEARING

The flywheel charge motor is connected to the flywheel package through two separate gearboxes, which match the charge motor speed with the desired rotor speed. The charge motor synchronous speed is 1,800 rpm. The flywheel fully charged speed is 16,700 rpm. A low-speed gearbox is coupled to the charge motor and a high-speed gearbox connected to the rotor package.

The low-speed gearbox is a chain-driven gearing system, which accomplishes the first speed increase through a transfer case at the charge motor output shaft. Figure 8 shows the transfer case and is identified as the low-speed gearbox. The transfer case steps the 1,800 rpm charge motor synchronous speed to 5,000 rpm. The output of this gearbox is coupled to the high-speed gearbox by a gear coupling (fig. 9) custom designed for the flywheel-powered system.

The high-speed gearbox provides a speed increase from 5,000 to 16,700 rpm for the flywheel. An auxiliary pump output shaft is incorporated in the gearbox for driving the flywheel-powered system and the hydraulic pump. This stage provides a speed reduction from 16,700 to 3,142 rpm.

A paramount design feature of the gearbox is the incorporation of an overrunning clutch on the flywheel input drive shaft of the gearbox. This clutch disengages the charge motor and low-speed gearbox from the flywheel rotor when it is up to speed (16,700 rpm). The auxiliary drive remains coupled to the rotating flywheel and provides power to the system hydraulic lubrication pump.

## FLYWHEEL ROTOR SYSTEM

The flywheel system fits in a 34 by 28 in cross-sectional compartment normally occupied by the shuttle car cable reel. It is designed to deliver 4.5 kW·h of usable energy and a total energy storage capability of 6.22 kW·h at 16,700 rpm. The flywheel module assembly is 27 in. in diam and 43.5 in long. The module consists of a cylindrical outer case with end plates and load bearing subassemblies at each end. A 23-in diam, seven-disk flywheel rotor is mounted horizontally within the case. Each disk weighs 741.8 lb for an approximate rotor weight of 5,193 lb. The rotor is surrounded by a braking ring and is supported by bearings at each end. Carbon-face shaft seals are located between the rotor chamber and the oil lubricated bearings. These seals provide for the application of a vacuum within the rotor case.

Safety with regard to rotor containment was a primary design factor of the flywheel module. At full speed, the flywheel would have considerable energy that, if suddenly released, would cause significant damage. The rotor is designed to prevent explosive failure. Figure 10 shows the mechanical fuse concept built into each of the seven-rotor discs. If the rotor contacts the case with significant force, then the rim will break around the neck area and contact the stationary braking ring attached to the flywheel case and stop the rim. The rotor hub would retain sufficient balance and come to a stop without major damage.

A constant-stress principle was used to design the rotating disks, which is based on the physical characteristic

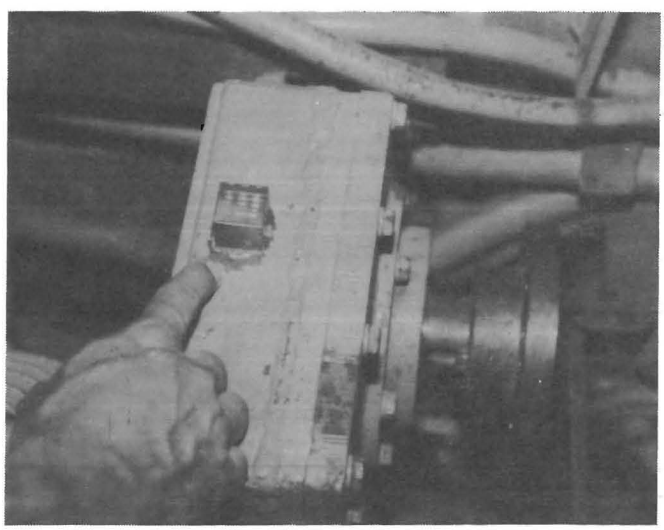

Figure 8.—Low-speed gearbox.

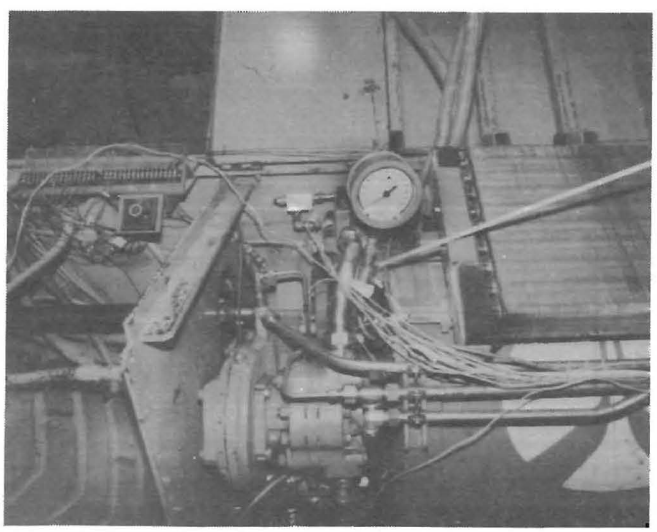

Figure 9.—Gear location in car.

that the stored energy in any element of the disk is proportional to the stress in the element. It follows that to achieve maximum energy storage, every element in the flywheel should be equally stressed to its maximum usable limit. The classical formula for a thickness of constant stress in a rotating disk is

$$Y = Y_a e^{-uw^2/2\sigma}$$

where $Y$ = the thickness at radius r, in,

$Y_a$ = thickness at the axis, in,

$u$ = material density, lb/in$^3$,

$w$ = angular velocity, rpm/s,

$r$ = distance from the axis, in,

$e$ = natural log,

and $\sigma$ = stress, psi.

Geometrical development of this formula results in a shape of gradually decreasing thickness that theoretically approaches zero as the radius approaches infinity.

It was recognized that a safer flywheel could be developed by some modification of the constant-stress shape. A reduced section near the outer rim combined with an enlarged rim shown in figure 10 results in a defined zone of increased stress. Because the high-stress zone is near the outer rim of the flywheel, failure of the disk causes the rim to breakaway reducing stress levels throughout the disk and prevents a far more dangerous failure.

The next principle adapted from existing technology was a method of attaching the hub without using center holes shown in figure 11. This reduces the stress by as much as a factor of 2 over a disk with a center hole. The flywheel disks are an optimization of the basic principles of constant-stress and hub attachments, designed using computer assisted finite element analysis and selection of high quality material.

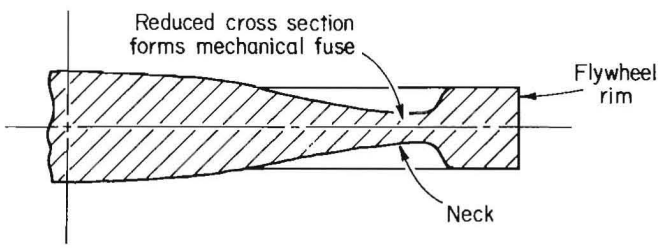


**Figure 10.—Mechanical fuse.**

## FLYWHEEL LUBRICATION AND HYDRAULIC SYSTEMS

The flywheel module requires lubrication for the bearings and operation of the vacuum pump and cooling fan. Figure 12 shows a schematic of the lubrication system on the flywheel module. The working fluid is automatic transmission fluid. The choice of lubricant was quite critical. Viscosity has a strong effect on bearing and gear life and the damping effect of the special squeeze film bearings used to prevent shaft dynamic problems. The oil should not age for several years at 1,200° to 1,500° F and vapor pressure must be under 0.02 psia (1 torr) to prevent overloading of the vacuum pump.

## VACUUM AND WINDAGE

To minimize air turbulence affects on the seven-rotor flywheel assembly, the flywheel housing must be kept at a partial vacuum. The vacuum pump is driven via a hydraulic motor and evacuates the rotor case to 0.2 psia (10 torr) or below, which is the point at which air turbulence can start to affect rotor performance. The vacuum pump adjacent to the flywheel package will evacuate 300 L/min. This will evacuate the housing to 0.2 psia (10 torr) in 4.5 min and reach and maintain 0.02 psia (1 torr) in 7 min.

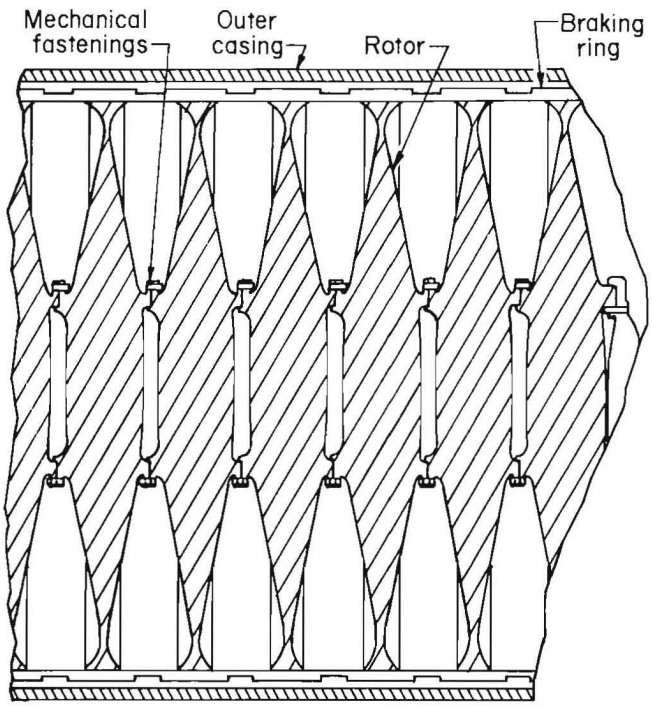


**Figure 11.—Rotor connections.**

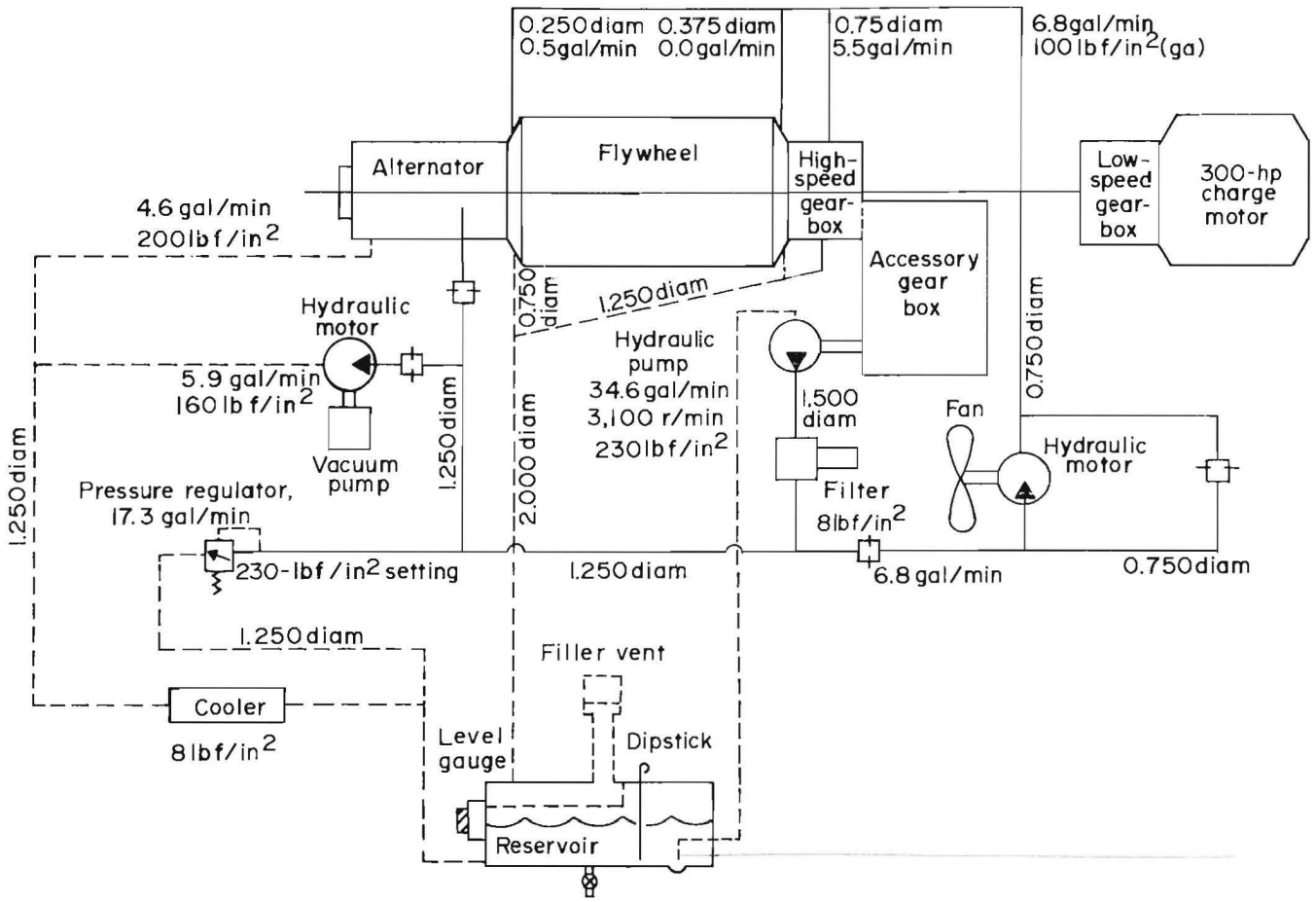


**Figure 12.—Hydraulic system. All diameters are in inches.**

The housing must make a vacuum tight container. Stresses due to the vacuum are very low because of the amount of metal required by rotor containment. However, the ends of the container must be convex to reduce deflections caused by the vacuum.

## ROTOR CONTAINMENT

At full speed, flywheel rotors contain a considerable amount of energy (21.6 J), the sudden release of which could result if a failure occurs. Thus, for safety reasons, a rotor containment system is needed. The rotor system used is shaped so that an explosive failure is almost impossible; instead, the rotor rim will break around the neck area and contact an internal breaking ring which will stop it. The breaking ring and housing are designed to contain the fragments should this occur.

Another type of failure which could occur is the "dropped rotor case", which occurs as a result of shaft or bearing failure, including loss of lubrication. In this case, the rotor rubs the braking ring at very high speeds and will be stopped by friction without developing excessive force. The total energy to be absorbed would be 6 kW·h or less and is designed to be absorbed by the 2,400 lb of steel in the containment housing.

## DIRECT CURRENT GENERATOR

The generator selected to convert the flywheel inertial energy into usable electrical energy was a compact power generator designed for efficiency at the operating speeds of the flywheel rotors. This allowed the generator to be directly attached to the flywheel, eliminating the gear losses that would be anticipated otherwise. The purpose of the generator system is to supply 270-V dc power to the shuttle car's normal electrical circuitry up to a limit of 45 kW with an operating range of 8,500 to 16,700 rpm. The generator is a wound-rotor, nonsalient pole, synchronous, brushless generator. It has an integral ac exciter, rotating rectifiers, permanent magnet generator, and a double-bridge rectifier system with interphase transformer to convert the ac generator's output to dc. Excitation for control of the generator's output voltage is supplied to the rotating field of the main generator by the ac exciter

through the exciter rectifiers. The permanent magnet generator (PMG) furnishes the power for the exciter and system control functions.

The generator package is mechanically connected to the flywheel that spins from 0 to 16,700 rpm, but is operable only between 7,500 and 16,700 rpm. The generator output can be enabled or disabled depending on whether or not the excitation field is energized, and also on the amount of excitation. This control feature facilitates output voltage regulation, current regulation, and emergency shutdown should a condition arise on the car that is potentially detrimental to the generator system.

### GENERATOR CONTROL UNIT

Control of the entire generator system is delegated to the generator control unit (GCU) as shown in figure 13. The GCU monitors vital generator parameters from which it adjusts to the exciter field current for regulation purposes. The GCU also monitors areas of potential faults that result in generator action shutdown. The GCU provides outputs that are interfaced to the ESD-supplied operator's monitoring station. This station warns of possible problems before a shutdown of the generator is required by the GCU. The monitoring station allows the shuttle car operator time to correct a problem before power to the car is lost. If delivered power is shutoff by the GCU, then the operator can ascertain why the shutdown occurred via the monitoring station read outs. Once the generator system is up to speed, power is supplied by the generator to run the normal shuttle car functions until the flywheel system has to be recharged.

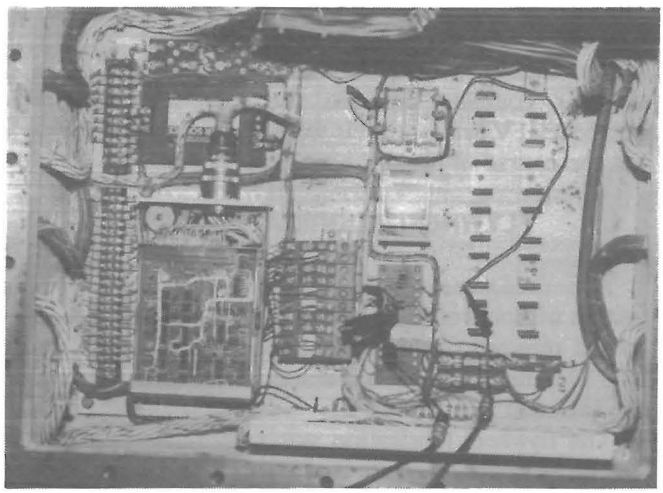

**Figure 13.—Generator control unit.**

## SURFACE TESTING

### TEST PROGRAM OVERVIEW

The objectives of the surface testing were to verify the capability of the flywheel energy storage package to power the shuttle car over a nominal coal mine face haulage duty cycle and to evaluate the shuttle car's worthiness for an underground demonstration. The FPSC as received at a Bureau facility had never operated successfully. A test plan was generated to address the unresolved problems and the requirements document objectives. The test plan took an extremely cautious approach because the major system components were prototype devices that could not be replaced.

### STARTER VERIFICATION TESTS

Tests were designed to determine the operating characteristics of the solid-state starter before energizing the shuttle car's 300-hp charge motor. The objectives were to become familiar with operation of the solid-state starter, install instruments that would remain in use as the test program progressed, and to determine the calibration of the starter adjustments. Each of the starter parameters was evaluated (current limit, current trip, ramp time, and initial voltage). Appendix A documents the results of the starter verification tests. It was determined that the calibration of the starter adjustments was sufficient to permit successful operation of the equipment.

### CHARGE MOTOR VERIFICATION TESTS

The next sequence of testing involved the evaluation of the charge motor interfaced to the solid-state starter. The intermediate drive shaft between the low-speed transfer case and the high-speed gearbox was removed. Removal of this shaft enabled the charge motor and low-speed transfer case to be operated without powering the flywheel. Appendix B contains the details of the tests conducted. The charge motor, starter, and transfer case operated as expected. Proper rotation and speed of the motor and transfer case were verified (counterclockwise when looking at the shaft end at 1,800 rpm).

However, a significant visible wobble was observed in the Morse transfer case. This wobble was considered detrimental to the system operation. Through testing reported in appendix B, it was determined that resonance frequencies of the transfer case were being created by vibration of the bull and pinion shaft caused by misalignment and unbalance shaft forces. A stiffener was added between the charge motor housing and the transfer case.

The stiffener not only increased transfer case natural frequencies, but aided in maintaining alignment. Additional system stiffness would be obtained with the addition of the gear coupling between the low- and high-speed gearboxes. Vibration levels would be monitored throughout the course of the test program.

## FLYWHEEL LUBRICATION TESTS

A method was devised to power the flywheel lubrication system without rolling over the flywheel. This method required removal of the flywheel package from the shuttle car. Details of the test apparatus, procedures, and results are included in appendix C.

The flywheel lubrication system requires precise flow and pressure for lubrication of bearings and other mechanical components. The vacuum pump and cooling fan are also driven by the lubrication system.

Initial testing of the lubrication system revealed several problems. The system reservoir was contaminated, and the access cover was poorly designed. The reservoir was cleaned and the access cover modified (see appendix C). The hydraulic pump was installed with the pressure and return ports reversed. Initial activation of the pump resulted in no flow. This nonflow condition would have resulted in a major disaster if this error had not been detected and the flywheel was rotating. Upon replumbing the pump and activation of the lube system, a major leak was found in the generator. This leak was the result of collapsed seals in the generator. If this leak would have occurred while operating the flywheel, then a major mechanical problem would have developed due to lack of lubrication. The lube system has a 7-gal reservoir and the 17-gpm pump would have depleted the fluid supply quickly. Subsequent operation of the system with repairs and modifications confirmed proper operation of the system.

An anomaly was noted in the hydraulically driven vacuum pump system. Without initial vacuum in the flywheel housing, the vacuum pump and lubrication system operated as expected. However, when the lubrication system was operated with an initial vacuum in the flywheel housing, the vacuum pump was locked up due to the high torque requirements imposed by the flywheel vacuum on the vacuum pump drive. This situation caused a change in the flow characteristics of the lubrication system (see appendix C), and was remedied by installing a bleed valve in the flywheel housing. This valve allowed the flywheel housing vacuum to bleed off prior to energizing the lubrication system.

## GENERATOR CONTROL CIRCUITRY CONTINUITY TESTS

This circuitry contains the GCU relays that indicate generator status in the event of a fault and related support circuitry. The circuitry can be divided into four groups: the 28-V dc system, the 5-V dc system, the 15-V dc system, and the GCU.

The 28-V dc system is powered by the GCU and the PMG. The circuit contains the relay that enables the main contractor to apply power to the normal car functions. This part of the circuitry also contains the battery circuit that supplies instrumentation and indicator circuitry power during flywheel charging.

The 5-V dc supply is powered by the 28-V dc system. This system contains the fault-indicating relays and associated readout devices located in the operator's station. This system directly interfaces with the GCU's fault detect circuitry.

The 15-V dc system is powered from the 5-V dc supply. The function of this system is to supply operating power to the instrumentation amplifiers, monitoring rotor speed, oil pressure, oil and case temperatures, generator amps, and volts.

The GCU is powered by the PMG and is interfaced to the stock shuttle car electrical system (fig. 14). The function of the GCU is to provide control for the main generator and to detect fault conditions. The GCU contains electronic circuits that perform the following functions.

1. Rectify PMG output for use in field excitation of the main generator and supply power for control and fault detect electronics.
2. Monitor generator voltage, current, and alter field excitation as required.
3. Monitor voltage, current, temperature, and ground integrity, and shutdown generator action should values exceed preset limits.

Phase 1 of circuitry testing was accomplished on a point-to-point basis using an ohmmeter to verify that the circuitry was connected as designed. A discrepancy was found in the 28-V dc system. The return for the 28-V dc supply of the power relay was not connected in the main contactor case. TD1, which is the time delay module for the battery powered relay, was not installed. Spare TD units were tested, and one was installed to verify circuit operation. All other systems were operationally correct according to schematics.

Phase 2 of testing involved the application of power to the circuitry components. With the application of power, various fault conditions were simulated to ensure the circuitry performed as intended. The following fault conditions were simulated: ground fault, overvoltage, overcurrent, generator overtemperature warning, and generator overtemperature trip.

The 28-, 5-, and 15-V dc systems showed all relays operating properly when fault conditions were simulated as originating in the GCU. The GCU can only be checked out with a three-phase power simulator. Appendix D describes the apparatus, procedure, and test results for the tests conducted on the GCU. The GCU unit failed the first time it was powered up and was modified and repaired in-house. After repair, it functioned properly.

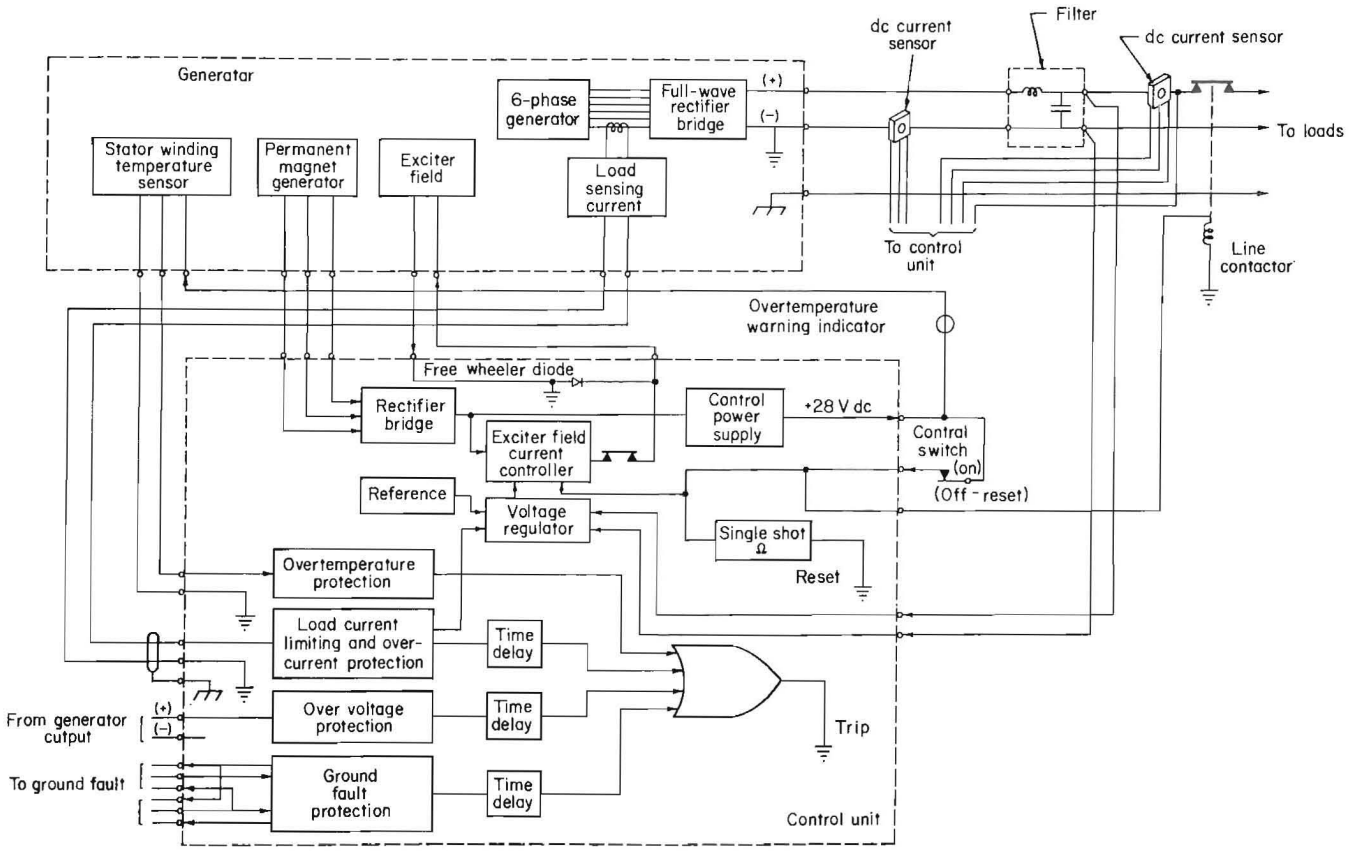


**Figure 14.—Generator control unit and permanent magnet generator.**

## SPIN UP OF FLYWHEEL WITHOUT GENERATOR

The first spin up of the flywheel assembly was performed without the generator attached. The flywheel package without the generator was fully instrumented and assembled on the shuttle car. Through testing it was determined that a current limit of 850 to 900 A was required to spin the flywheel up to full speed. Details of the testing and analysis are included in appendix E. This testing showed that the lubrication system and vacuum systems all functioned within acceptable limits. It was determined that there are at least two flywheel critical speeds at 4,800 and 10,680 rpm, and the squeeze film dampers provide adequate damping of the flywheel rotor vibration for normal duty cycle operation.

Charge time required to spin the flywheel up from 0 to 16,700 rpm was 5 min 1 s. Coast-down time to 8,400 rpm was on average 30 min 20 s. Recharge time from 8,400 to 16,700 rpm was 1 min 44 s. Total time to coast down from 16,700 to 0 rpm was 89 min 35 s.

The charge motor is marginal with regard to internal winding temperature. The charge motor has nearly reached temperature limit when the system reaches full speed. The cool-down period is dependent on ambient air temperature. If cool down does not occur to a significant degree during the shuttle car duty cycle operation, the motor will overheat during the recharge cycle of 8,500 rpm to 16,700 rpm. This temperature problem could be resolved by using a different class-duty cycle motor better matched to the flywheel package charge requirements.

Sound level measurements were obtained 3 ft from the side of the flywheel housing while the flywheel was at 16,700 rpm. A reading of 100 dB was measured. The covers were not installed when this measurement was taken, and when installed, the level will decrease.

These tests constituted the first major milestone in the testing and evaluation of the FPSC. The flywheel was successfully brought up to full speed. Preparations for a flywheel spin up with the generator were immediately implemented.

## SPIN UP OF FLYWHEEL WITH GENERATOR AND RESISTIVE LOAD BANK TESTS

The next sequence in the test program involved resistive load testing of the generator when spun up to full speed. This testing represented another major milestone in the test program. All flywheel package systems would

be operational, except for the final interface of the generator to the shuttle car power control circuitry. A resistive load bank circuit was designed and installed in the shuttle car conveyor. Figure 15 shows the resistive load bank installation in the shuttle car conveyor. Appendix F contains details of the test apparatus and test results. All flywheel systems functioned within operating limits. Test results indicate that the flywheel power package should provide sufficient power to complete the theoretically proposed duty cycles. However, it does not appear that there will be the reserve energy originally expected until a more efficient electric system is assembled. Appendix F shows the development of an empirical equation for determining flywheel speed change due to the load applied at the generator output.

## FLYWHEEL POWER PACKAGE INTERFACED TO SHUTTLE CAR POWER CONTROL CIRCUITRY

This test involved the interface of the output power leads of the generator to the shuttle car. The objective of the testing was to verify operation of the shuttle car via power supplied by the flywheel power package. The flywheel was brought up to 16,700 rpm via the charging system. The generator was activated, and the lighting system turned on successfully. The electric motor driving the shuttle car hydraulics was then activated. Portions of the GCU circuitry failed immediately. This phase of the test program was aborted, and an investigation of the failure was initiated along with repair of the damaged electronic circuitry.

The shuttle car is designed with large values of capacitance and inductance of sufficient charge to filter line variations in typical mine power centers. Approximate values are 1,000 $\mu$F per 500 V dc capacitance and 12 $\mu$H inductance. These devices require large instantaneous amounts of power to initialize or charge them. Testing, using the 270-V dc power center interfaced to the machine after the failure, showed an instantaneous current reading of approximately 400-A dc when the main line contactors are closed.

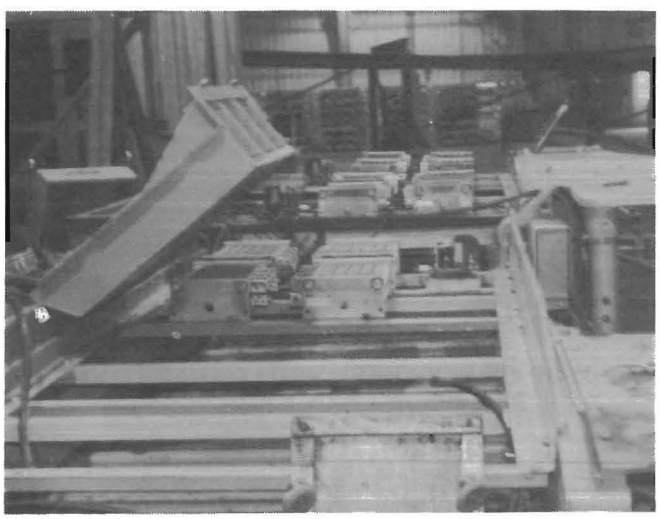

**Figure 15.—Resistive load bank.**

Review of the frequency modulation (FM) tape recorded data for the test showed that portions of the GCU error regulation circuitry may have failed or been inoperative prior to the test. The generator began a run away sequence until the overvoltage circuit disabled field excitation and all outputs went to zero. Appendix G contains the results of the failure analysis conducted.

Problems were traced to the generator control system's lag time in response to apparent loads. This lag time is due to the required charge time of the excitor field once the control electronics have interpreted an increase in the load. The electronics cause an overshoot of the generator output when a transient load condition analogous to the pump activation is encountered. This overshoot also occurs when a load is released because there must be a dissipation of the excitor field power before the generator output can come into compliance with the load demands. The shuttle car power circuitry also caused transient voltage spikes detrimental to the generator control electronics. It was also apparent that the inherent waveforms generated by the SCR chopper system for traction motor speed control, when coupled to the response time of the GCU, could cause a resonant oscillation in the control circuitry of the GCU. This resonance would have an adverse effect on system stability.

From the resistive load test data it was determined that the overshoot phenomena observed when engaging or disengaging loads was diminished when there was an initial static load attached to the output of the generator. The 5-kW resistive load bank would be utilized to maintain the static load condition. The capacitors and inductors, which provided filtering, would be removed to eliminate the transient caused by these devices. The SCR traction motor speed control would be replaced with a simplified contactor speed control circuitry available from an identical shuttle car. Resistors would be added in series with the traction motors so that transients associated with motor activation would be limited to 125 A dc. The total instantaneous power requirement of the shuttle car would be limited to 45 kW. Finally, since problems were encountered with the operator's station monitoring panel, the panel and signal conditioning was disconnected from the GCU circuitry.

On 5 August 1987, the FPSC trammed 10 ft under flywheel power. The machine could not be trammed further due to the instrumentation umbilical attached to monitoring electronic instrumentation. On 20 August 1987, provisions were completed for mounting and powering of

all electronic hardware on the shuttle car. The shuttle car successfully trammed over 800 ft under flywheel power. Appendix G contains details of the test, data obtained, and test results.

These tests have proven the shuttle car can be operated under flywheel power. There were no gyroscopic effects due to the flywheel rotation detrimental to the steerage of the shuttle car. The major drawback noted was that the maximum obtainable tram speed was approximately 1.2 mph. This speed had a detrimental effect on the ability of the shuttle car to complete duty cycle requirements. The duty cycle proposed in appendix F calls for 4-mph tram speed empty and 2.7-mph tram speed loaded. The generator can deliver the necessary power, but the current generator to shuttle car interface was inadequate. Optimization of this dynamic interface required additional engineering investigation and testing.

The FPSC was retrofitted with a solid-state control circuit that increased efficiency by 33 pct. A new interface was designed to compensate for generator-control system lag time in response to apparent loads, which had caused generator problems when initializing the system. The use of a solid-state traction drive system also allowed variable control of the tram circuit replacing the on-off type of operation that was previously on the machine. Results from surface testing indicate that the solid-state circuitry will increase the tram rate from 1 to 4 mph.

The FPSC was surface tested in a mockup path that simulated an underground duty cycle carrying a full load of coal. Results from surface testing indicate that an average speed of 3.5 mph was achieved, thereby making the FPSC competitive with conventional shuttle cars with trailing cables and satisfying the original design specifications.

## CONCLUSIONS

The shuttle car, as originally configured with regard to the generator and shuttle car power interface, could not fulfill mine duty cycle requirements. The electrical configuration currently installed took a fail-safe approach to this most important interface. This approach was successful and proved that the shuttle car could be operated via a flywheel power system. There were no gyroscopic effects on the vehicle handling from the flywheel rotor.

To accomplish the duty cycle simulation phase of the test program, the generator to shuttle car power interface needed to be optimized. This optimization required additional engineering and testing to ensure the shuttle car can complete a mine duty haulage cycle.

The FPSC was retrofitted with a modified solid-state control circuit and interface circuit between the control circuit and the GCU. These system changes increased the efficiency by 33 pct. In addition, the solid-state circuitry allowed variable control of the tram circuit, which replaced the on-off type operation that was previously on the machine. Results from the surface testing indicate that the solid-state circuitry will increase the tram rate by 1 to 4 mph, thereby satisfying the original design specifications. The final surface test was the completion of a typical mission duty cycle with a typical load of coal. The shuttle car was able to complete the duty cycle at an average speed of 3.5 mph, thereby making it competitive with conventional shuttle cars with trailing cables.

The FPSC was designed and fabricated to increase productivity in underground coal mines by determining if flywheel power technology, applied to shuttle cars, could provide a reasonable alternative to the conventional shuttle car powered by an electric trailing cable. This alternative to conventional power cable systems consists of the world's first seven-rotor stacked flywheel system capable of storing 6 kW·h of energy at 16,700 rpm. The FPSC was designed on the chassis of a standard shuttle car and has the capacity to complete one duty cycle on one charging of the flywheel.

The surface tests have proven that the flywheel energy system can function and operate the shuttle car. Gyroscopic effects were insignificant with regard to vehicle steerability. The newly designed interface between the generator and the solid-state traction drive system has been successfully surface tested. Results indicate that the original design specification of 3.5 mph (see appendix G for averages) has been achieved which permits the FPSC to complete a typical duty cycle underground before recharging. No economic studies of such a system were included in the project.

A remote charging station is being designed with finite element analysis that will analyze the dynamic loading interface between the charging station and the FPSC. The remote charging station will reduce vehicle weight and permit the use of a more efficient charge motor. The most promising concept has the shuttle car being recharged while discharging coal at the section belt by an automatic docking mechanism, which locks onto the FPSC and spins the flywheel up to 16,700 rpm.

# APPENDIX A.—STARTER VERIFICATION TEST

## Setup and Instrumentation

To verify operation of a solid-state starter, the unit was connected to a chain conveyor system which provided a suitable load.

The voltage, current, and power supplied to the conveyor motor was measured at the starter output terminals. A two-element watts transducer measured total motor power. A voltage transducer monitored line to line voltage and a current transducer detected phase current. Current and potential transformers were selected to enable the transducers to operate within their measurement range. Each transducer produced a 1-V full-scale analog signal, which was recorded on a strip chart.

## Test Procedure

Each of the starter parameters was adjusted to various settings throughout their ranges, while all other controls remained fixed. The following are the four starter adjustments.

1. *Current Limit* - Determines the maximum current draw that the motor is permitted. The reduced current capability prevents the motor from imposing excessive output torque. This control is adjustable from 75 to 300 pct of the motor's full-load current rating.

2. *Current Trip* - Turns off the starter and lights a red indicator when a running overload has occurred. A 40-s time delay after the start command enables the motor to come up to speed before the trip becomes active. The trip can be set between 75 and 150 pct of the motor's full-load current rating.

3. *Ramp Time* - Selects the rate of linear voltage increase until full-line voltage is reached. A current limit override may extend the ramp time. The control is adjustable from 1 to 30 s.

4. *Initial Voltage* - Sets the initial voltage to a level that enables the motor to exceed breakaway torque when it is first started. The adjustment can vary the initial voltage from 0 to 50 pct of line voltage.

A start was initiated and the strip chart recorded the voltage, current, and power until the motor reached a steady-state condition. Figure A-1 shows a typical starting event. The peak current, ramp time, and initial voltage were determined for each start.

## Results

A total of 11 starts were made at various control settings. Table A-1 shows a reduction of the data taken from the strip chart and observations made during the tests. Trials 1 to 3 determine the accuracy of the ramp time adjustment, and trials 4 to 6 check the response to the initial voltage adjustment.

Figure A-2 illustrates the calibration of the ramp time, current limit, and initial voltage controls. The dashed line represents the calibration expected as described in the starter operator's manual.

Based on the results of these operational checks, the following conclusions can be made:

1. The calibration of the starter adjustments is sufficiently consistent with the operator's manual description to permit successful operation of the equipment.

2. The initial voltage is affected by changes in the ramp time and current limit. Therefore it should be set last.

3. An oscillation in motor torque of approximately 2.2 Hz was observed just before the motor reached full speed. This may be related to the mechanical load characteristics of the conveyor system.

4. A current trip condition could not be duplicated with this test setup.

**Table A-1.—Data from solid-state tests**

| Trial | Current limit setting, A | Current trip setting, A | Ramp time setting, s | Initial voltage setting, V ac | Peak motor current, A | Indication of trip | Ramp time, s | Initial voltage, V ac | Comments |
|---|---|---|---|---|---|---|---|---|---|
| 1 | 872 | 315 | 21.3 | 55 | [1]540 | None | 25 | 103 | None. |
| 2 | 872 | 315 | 30 | 55 | [1]520 | do. | 32 | 71 | Do. |
| 3 | 872 | 315 | 1 | 55 | 590 | do. | 3 | 309 | Do. |
| 4 | 1,200 | 315 | 1 | 55 | 960 | do. | 1 | 431 | Do. |
| 5 | 300 | 315 | 1 | 55 | 200 | do.[2] | (3) | 185 | Motor failed to accelerate. |
| 6 | 570 | 315 | 1 | 55 | 400 | do. | [3]17 | 252 | Motor slow to accelerte. |
| 7 | 570 | 300 | 1 | 55 | 400 | do. | [3]14 | 252 | Do. |
| 8 | 1,200 | 300 | 30 | 55 | [1]550 | do. | 33 | 103 | Motor turned after 2.1 s. |
| 9 | 1,200 | 300 | 30 | 0 | [1]514 | do. | 30 | 0 | Motor turned after 4.6 s. |
| 10 | 1,200 | 300 | 30 | 234 | [1]716 | do. | 25 | 354 | Motor turned immediately. |
| 11 | 1,200 | 300 | 30 | 96 | [1]502 | do. | 32 | 148 | Do. |

[1]Current did not reach saturation.
[2]Over-current condition was not held long enough for trip.
[3]Ramp time was extended by current limit.

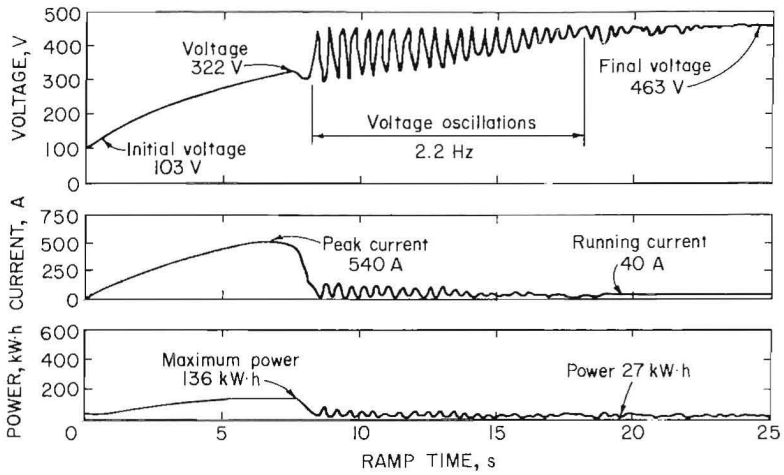


**Figure A-1.—Typical starting event.**

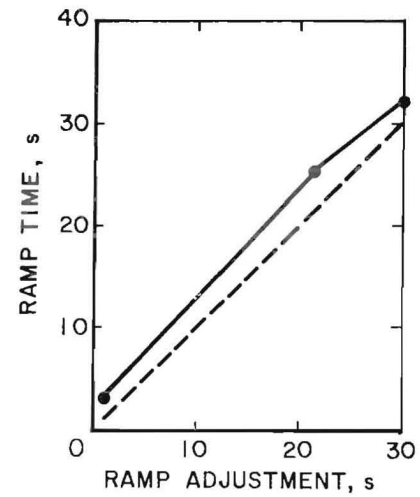


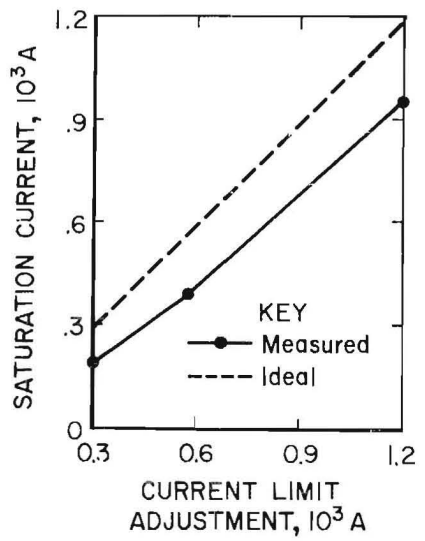


**Figure A-2.—Calibration of ramp time.**

# APPENDIX B.—CHARGE MOTOR VERIFICATION TEST

## Setup and Instrumentation

To verify operation of the solid-state starter and charge motor, the same measurement circuit described in appendix A was used. Voltage, current, and power were measured at the same test points used in the charge motor verification testing. The intermediate drive shaft between the low-speed transfer case and the high-speed gearbox was removed to isolate the charge motor from the flywheel package. A magnetic pickup (fig. B-1) was installed on the low-speed shaft of the transfer case to sense charge motor speed. The pickup would generate a one pulse per revolution signal, which was connected to a frequency counter to give a speed readout. Additionally, three accelerometers were used to monitor vibration of the charge motor and transfer case (fig. B-2).

## Test Procedure

The 300-hp charge motor was electrically connected to the solid-state starter. All instrumentation systems were activated, and the start button was engaged on the solid-state starter. The motor was allowed to come up to full speed of 1,800 rpm, and remained at that speed until the stop button on the solid-state starter was activated. The motor and transfer case would then coast down to a stop. This procedure was repeated several times with the accelerometers mounted at different locations on the charge motor and transfer case.

## Results

The loads imposed on the charge motor with the intermediate drive shaft removed were insufficient for evaluating motor and starter characteristics. Proper rotation and speed of the charge motor were verified (counterclockwise when looking at the shaft end at 1,800 rpm).

A significant visible wobble was observed in the Morse transfer case when the motor was operating. Spectrum analysis of the tape recorded accelerometer data was undertaken to evaluate the cause of the vibration, since it could be detrimental to the flywheel package hardware.

International Standards Organization (ISO) standard 3945 was used as a guideline for vibration severity judgement. A severity criteria of 0.25 in/s and greater was chosen as the unacceptable range because the standard

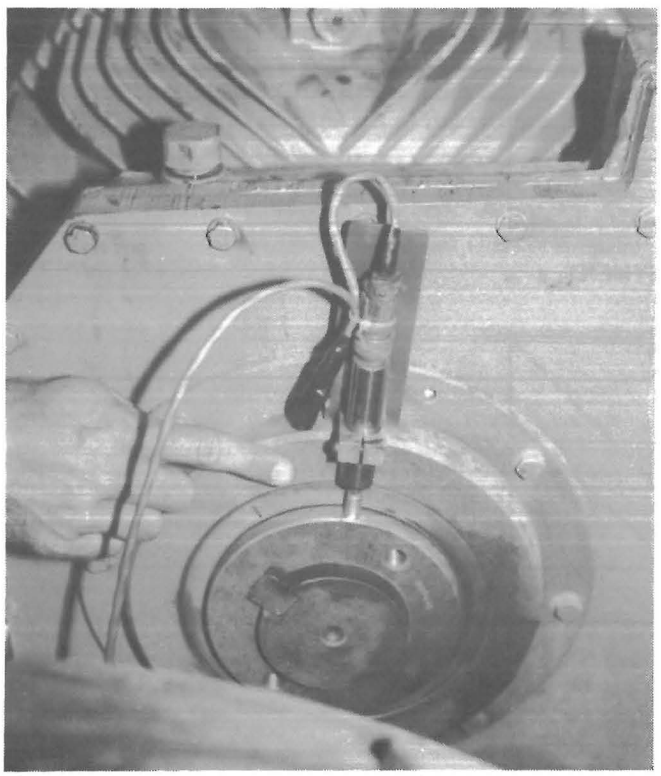

Figure B-1.—Magnetic pickup.

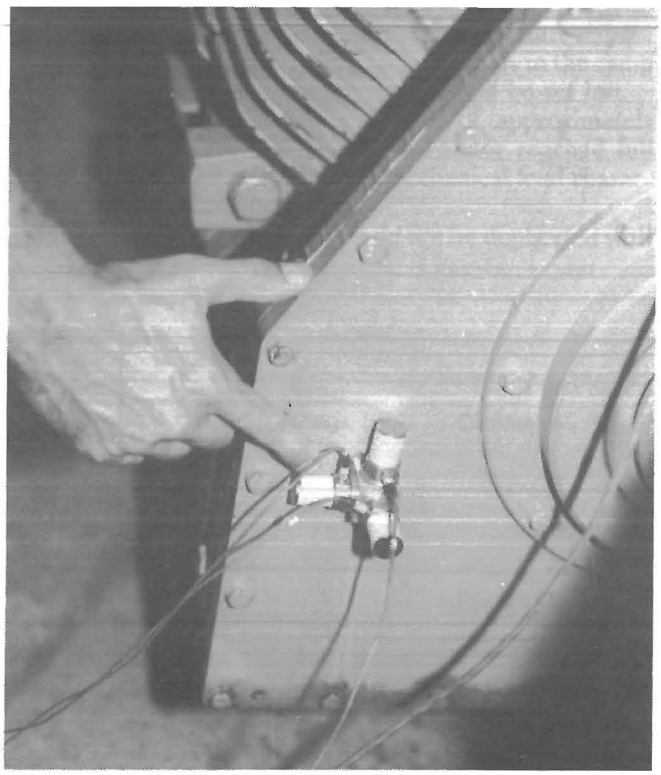

Figure B-2.—Accelerometer placement.

establishes this level as being unsatisfactory for hard and soft supported gearcases.

Peak hold spectrum plots were generated using a spectrum analyzer for acceleration measurements at various locations on the charge motor and transfer case. The peak hold mode of operation records the highest value for any frequency while the analyzer is operational. Since these spectrum plots were generated while the machinery coasted down from full speed condition to zero speed, a continuous record of running speed frequency and amplitude was generated. Figure B-3 is a typical peak hold acceleration plot generated for the transfer case in the axial direction. Table B-1 tabulates those frequencies that are theoretically associated with the rotating shaft components at full running speed. Typically, rotating shaft unbalance vibration is characterized by increasing vibration amplitude with increased running speed frequency by the following force equation,

$$F = MRW$$

where F = force, M = unbalanced mass, R = radius of mass unbalance from center of shaft rotation, and W = running speed, radians per second.

**Table B-1.—Running speed frequency components**

| Associated hardware | Speed, rpm | Harmonics, Hz | | | | | |
|---|---|---|---|---|---|---|---|
| | | Base | X 2 | X 3 | X 4 | X 5 | X 6 |
| Charge motor . . . . . | 1,800 | 30 | 60 | 90 | 120 | 150 | 180 |
| Morse transfer case: | | | | | | | |
| Slow-speed shaft . . | 1,800 | 30 | 60 | 90 | 120 | 150 | 180 |
| High-speed shaft . . | 5,000 | 83 | 166 | 249 | 332 | 415 | 498 |

NOTE: Multiplication factors show the frequencies that were monitored.

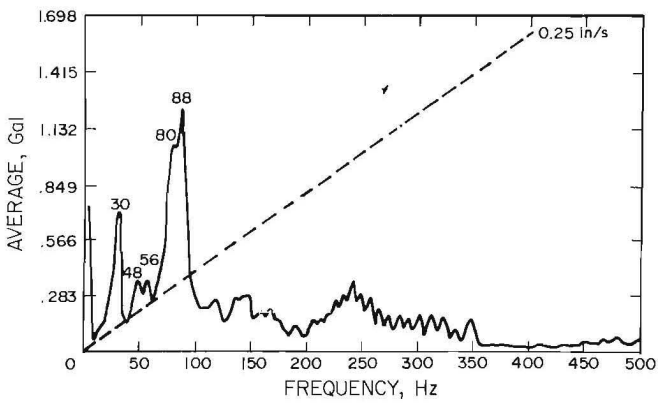


**Figure B-3.—Axial direction, top of transfer case, coast down peak hold acceleration.**

To distinguish between vibration due to shaft unbalance and structural resonances of the transfer case, rap tests were conducted on the transfer case. A rap test simply involves rapping the structure with a hammer and measuring the response with an accelerometer. Figure B-4 is a typical spectrum plot generated by rap testing. The frequencies shown in these plots represent the natural frequencies of the transfer case. Table B-2 tabulates these natural frequencies. Table B-3 tabulates those frequencies in the transfer case which exceed the 0.25 in/s severity criteria. The data indicate that the bull and pinion shafts of the transfer case are exciting the transfer case structural resonances via unbalance or misalignment shaft induced forces.

**Table B-2.—Transfer case structural resonance frequencies, Hertz**

| Sampling location . . | 1 | 2 | 3 | 4 | 5 | 6 |
|---|---|---|---|---|---|---|
| Axial . . . . . | 20 | 44 | 84 | 112 | 170 | 268 |
| Lateral . . . . . | 39 | 46 | 74 | 98 | 106 | 157 |
| Radial . . . . . | 16 | 39 | 46 | 73 | ND | ND |

ND No data.

NOTE: Designations 1 through 6 represents the major peak frequencies.

**Table B-3.—Tabulated frequencies exceeding 0.25 in/s during coast down**

| Location and direction | Frequencies[1] | | | | | |
|---|---|---|---|---|---|---|
| | 1 | 2 | 3 | 4 | 5 | 6 |
| Top transfer case: | | | | | | |
| Lateral . . . . . | 30 | 56 | 70 | 83 | 86 | ND |
| Axial . . . . . | 30 | 48 | 56 | 80 | 83 | 86 |
| Radial . . . . . | 30 | 70 | 80 | 83 | ND | ND |
| Lower transfer case: | | | | | | |
| Lateral . . . . . | 30 | 70 | 83 | ND | ND | ND |
| Axial . . . . . | 22 | 30 | 60 | 83 | 86 | ND |
| Radial . . . . . | 30 | 46 | 74 | 83 | ND | ND |

ND No data.
[1]Peak frequencies.

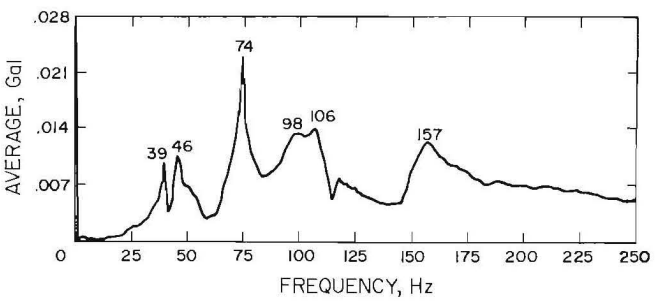


**Figure B-4.—Axial direction, bottom of transfer case, rap test.**

It was known that the stiffness of the transfer case would be altered when the intermediate drive shaft between the low-speed gearbox and high-speed gearbox was installed. This shaft installation would cause the transfer case resonant frequencies to increase, hopefully, out of the running speed frequency range of the rotating shafts.

As a precaution to increase case stiffness and maintain shaft alignment, a stiffener was added between the charge motor housing and the transfer case. Figure B-5 shows the stiffener. Great care will be taken to check alignment in all directions when the intermediate drive shaft is installed. This stiffness modification and alignment precautions should reduce transfer case vibration when coupled to the flywheel package. The visible wobble was eliminated with the stiffener added. Acceleration measurements were monitored during the flywheel spin up tests and no notable problems were observed.

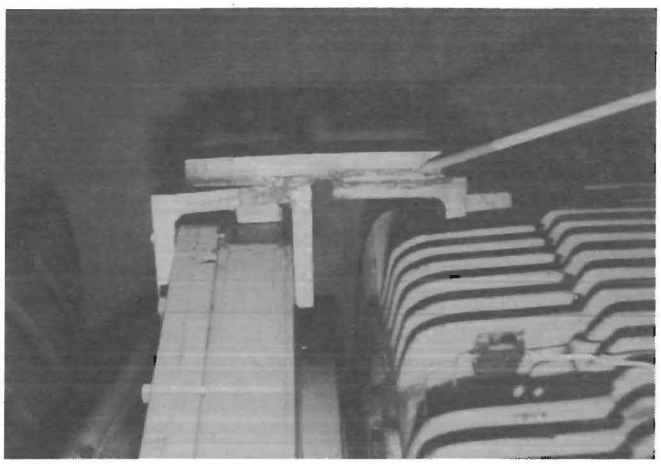

**Figure B-5.--Stiffener.**

# APPENDIX C.—FLYWHEEL LUBRICATION TEST

## Setup and Instrumentation

To verify operation of flywheel lubrication system, a test was conducted with the hydraulic system disconnected from the flywheel package. The hydraulic lubrication pump on the flywheel package is powered through the high-speed gearbox. This gearbox also interfaces the flywheel and normally turns simultaneously with the lubrication pump when the input shaft to the gearbox is rotated. The quill shaft interfacing the flywheel was removed so that the input shaft of the gearbox could be powered without rolling over the flywheel. With this shaft removed, the pump and lubrication system could be operated by supplying power to the input shaft of the gearbox. Figure C-1 is a detailed drawing of the gearbox. A belt and pulley system was devised to transfer power to the gearbox input shaft at 5,000 rpm using a 1,800-rpm electric motor. Figure C-2 shows the hardware configuration for powering the gearbox lubrication system.

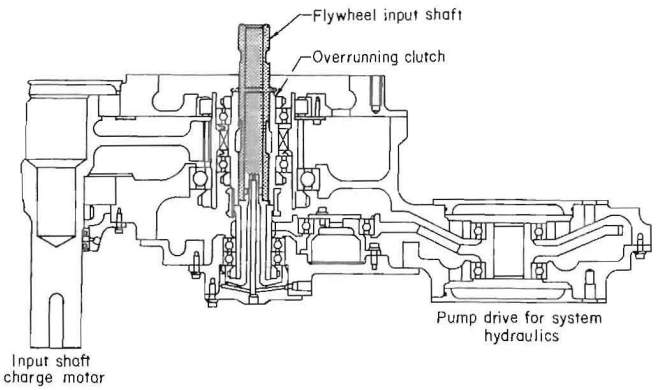


Figure C-1.—High-speed gearbox.

## Test Procedure

The first task undertaken regarding the lubrication system was to drain and clean the reservoir. Inspection of the reservoir revealed that a hole had been cut in the top to gain access. Duct tape was used to secure the cover. Since contamination of the lubrication system could result with this hardware, a new cover plate was fabricated. Figure C-3 shows the new reservoir and cover plate. The reservoir housing was drilled and threaded to accept sheet metal screws. A silicon gasket material was used between the cover plate and reservoir housing.

The next task undertaken was to remove the quill shaft from the high-speed gearbox and install the pulley drive system for power input to drive the lubrication pump. A pressure gauge was installed to monitor system pressure, and a vacuum gauge to monitor the flywheel housing vacuum. Turbine flow meters were installed in three locations of the hydraulic circuit. Power was turned on in order to drive the electric motor, and system parameters were evaluated, the flows and pressures are shown in the lube schematic.

## Results

When power was initially turned on to drive the gearbox, no flow was generated by the pump. It was discovered that the lubrication pump was installed with the suction and pressure ports reversed. This problem was corrected, and the lubrication system was again energized. A substantial oil leak was observed in the generator housing.

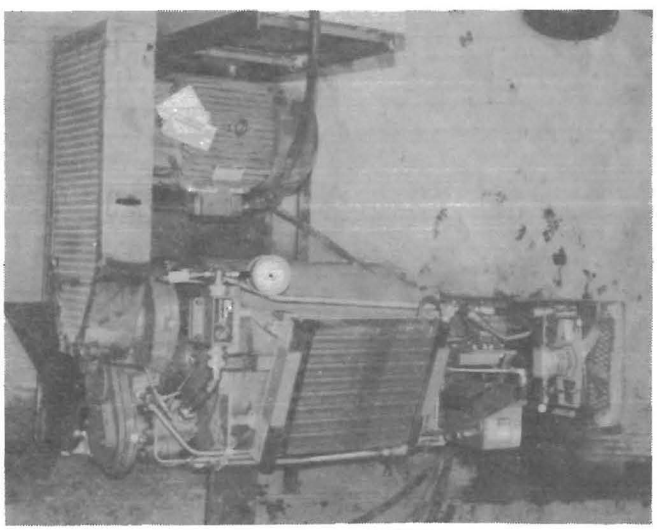

Figure C-2.—Hardware setup.

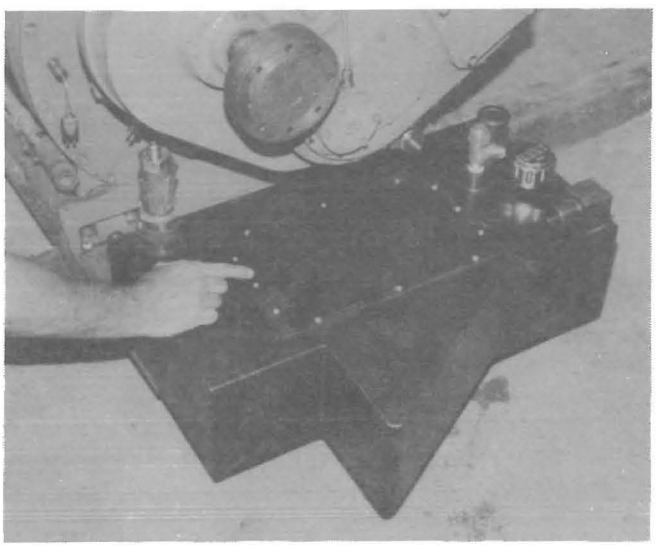

Figure C-3.—Modified hydraulic reservoir.

Figure C-4 shows where the oil leak occurred. Transmission fluid was leaking from the power discharge leads of the generator. Inspection revealed that the internal seals of the generator had collapsed and needed replacing. The generator was removed, and a Plexiglas acrylic plastic cover plate was installed on that end of the flywheel housing. This cover allowed further testing of the lube system while the generator was being repaired.

The lubrication system was replumbed, bypassing the generator circuit so that the system could be operated. A flow control valve was used to simulate flow characteristics of the generator. With the motor pulley system driving the hydraulic pump at 3,100 rpm, system relief pressure was adjusted to 230 psi and the flow control valve was adjusted to allow 4.6 gpm. With these pressure and flow adjustments, a 6.7 gpm bearing flow was verified. Subsequent operation of the system indicated no other leaks were present and that the fan motor and vacuum system would operate.

The generator was installed back into the test fixture after repair to verify proper flow through the generator circuit. Initial operation of the system showed that the return line coupled to the generator drainline was causing back flow through the generator drain port and flooding the bell housing of the generator enclosure. It was determined that the drain connection to the return line was not necessary since very little fluid was coming out of the drain port. Furthermore, the drain port only provided escape for any minimal leakage around the o-ring seals of the housing plate adaptor. With the drain port open to atmosphere operation of the lube system, the generator produced the required 4.6 gpm flow rate.

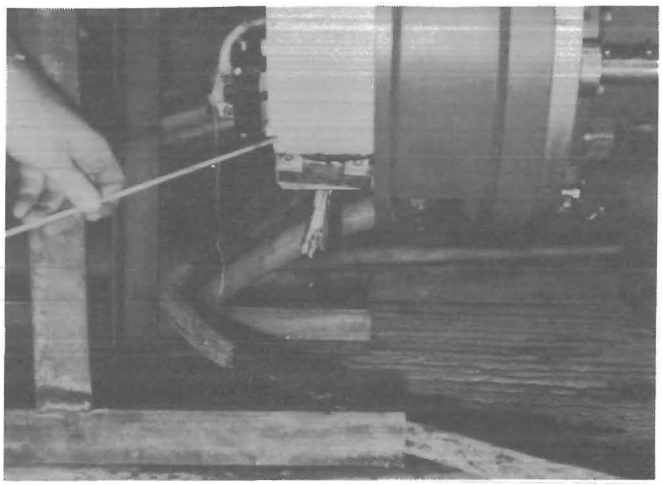

**Figure C-4.—Oil leak.**

An anomaly in the vacuum system was observed during lubrication testing. Initially, without vacuum in the flywheel housing, the hydraulic pump driving the vacuum pump would operate continuously and draw a vacuum. When the lubrication system was de-energized and re-energized with a vacuum in the flywheel housing, the hydraulic motor driving the vacuum pump would stall because of the differential pressure across the vacuum pump. This stalling caused system pressure to increase, and caused the flow to the generator branch of the circuit to decrease. If the vacuum was bled before energizing, the vacuum pump operated properly. This situation would be resolved by manually releasing the vacuum, and could be automated at a later time.

# APPENDIX D.—GENERATOR CONTROL UNIT TEST

## Setup and Instrumentation

The GCU monitors and adjusts key parameters of the 270-V dc generator unit. These parameters are generator output voltage, current, temperature, and ground system integrity. The purpose of this testing was to ensure operation of the GCU independent of the actual generator. The test required simulation of all inputs to the GCU from the generator unit and external sensing devices.

The first requirement of the GCU was power. This is normally accomplished by the PMG section of the generator package. The PMG supplies the GCU with a three-phase (ac) voltage that is rectified internally by the GCU to power the necessary electronic circuitry. To simulate the PMG for this test, a three-phase, variable autotransformer was incorporated into the circuit. Also contained in this circuit were a (dc) power supply used in place of the standby batteries and the high voltage dc power supply that would simulate the main generator output.

## Results

The GCU was supplied with power, and the internal power supplies operated normally for 5 min. The output of the internal power supplies went to zero, which indicated circuitry failure. At the same time, there was failure of one of the panel meters that indicated oil pressure located in the operator's station. Bench inspection of the GCU showed that the output voltage regulators had failed.

The failed components were the 15- and 28-V dc voltage regulators (fig. 14). The hybrid switching regulator (Q1), also failed and was designed to keep the input levels within acceptable levels over a wide range of supply voltages. The regulating function is basically accomplished by a pulse width modulator contained in the circuitry. Replacement components were installed. The GCU was powered up on the bench and allowed to run idle for approximately 4 h, while circuit checks were being made and documented.

The GCU was then reinstalled in the FPSC and powered up. The unit was allowed to run the machines' electronic systems in the idle mode without any problems. The systems functioning for this test were the internal electronic monitors, controls, and the external machine instrumentation installed by ESD Corp. The GCU operation now appeared normal.

# APPENDIX E.—FLYWHEEL SPIN UP WITHOUT GENERATOR

## Test Setup and Instrumentation

The objective of these tests was to become familiar with charging the flywheel up to full speed using all systems, except for the generator. The generator would be included in the next sequence of the test plan and removed the potential of damaging the prototype in the event of other system failures. This test sequence called for extensive instrumentation for measuring system parameters from which rapid engineering judgments could be made.

The flywheel package was installed on the shuttle car without the generator. A Plexiglass acrylic plastic plate and a flow control valve were used to accommodate this test without the generator (refer to appendix C). Twenty-six system parameters were instrumented for monitoring. These parameters would be used to evaluate the operating state of the system. A computerized, solid-state programmable controller was used to monitor and trigger alarms at preset levels. The user program interprets the input based in user instructions and either energizes or de-energizes output devices. Figure E-1 is a wiring schematic of the input and output parameters monitored and controlled by the processor. The indicated transducers were preconditioned with appropriate amplifiers and frequency-to-analog converters.

Using an industrial terminal supplied with a data acquisition system, a status report on lubrication, temperature, or vibration parameters could be displayed. Table E-1 tabulates the preset levels at which the program activated a horn and flashing light whenever any of the parameters exceeded the preset levels in minimum or maximum acceptable levels. This computer control system reduced a cumbersome amount of data channels into an easily handled data interrogation system with all data displayed in engineering units. The solid-state starter was also instrumented as defined in appendix A. A building block approach for instrumented parameters was maintained throughout the test program. A FM tape recorder was used to record selected parameters for post-test analysis. Table E-2 tabulates the parameters recorded.

## Procedure

The flywheel package without the generator was fully instrumented and assembled on the shuttle car. All systems were ready for the initial spin up of the flywheel. Current limit was set at 600 A. All strip charts and tape recorders were activated, and the controller was powered up. The test commenced with activation of the starter via a remote start switch. The area within 50 ft of the starter and machine was cleared of personnel for the first 10 s of activation because of the large current draw anticipated.

**Table E-1.—Operating parameters**

| Parameter | Range | Limit |
|---|---|---|
| Case vacuum . . . . . psi . . | 0.01-0.1 | 1 |
| Flow, gpm: | | |
| Main lube . . . . . | 10-17 | <10 |
| Alternator . . . . . | 2-6 | <1->8 |
| Bearing-gearbox . . . . . | 4-8 | <2->10 |
| Oil pressure . . . . . psi . . | 130-230 | <50 |
| Proximity probe rotor, in: | | |
| Axial . . . . . | 0-0.010 | [1]0.015 |
| Radial . . . . . | 0-1.010 | [1]0.015 |
| Rotor speed . . . . . rpm . . | 0-16,000 | 17,000 |
| Temperature, °F: | | |
| Flywheel housing . . . . . | 100-200 | 250 |
| Oil reservoir . . . . . | 130-200 | 250 |
| Flywheel bearings (4) . . . . . | 150-225 | 250 |
| Charge motor windings (6) . . . . . | 100-375 | 425 |
| Charge motor housing . . . . . | 100-200 | 250 |
| Vibration, Gal: | | |
| Gearbox . . . . . | 0-10 | [1]29 |
| Flywheel module . . . . . | 0-10 | [1]25 |

[1]Peak.

**Table E-2.—Data for flywheel spin up without generator**

| Channel | Parameter or sensor | Value |
|---|---|---|
| 1 . . . . | System lube pressure . . . . . psi . . | 250 |
| 2 . . . . | Flywheel vacuum . . . . . psia . . | 0.2 |
| 3 . . . . | Total flow . . . . . gpm . . | 17.2 |
| 4 . . . . | Bearing flow . . . . . gpm . . | 6.7 |
| 5 . . . . | Generator flow . . . . . gpm . . | 4.6 |
| 6 . . . . | Radial gearbox velocity . . . . . | NAp |
| 7 . . . . | Radial generator velocity . . . . . | NAp |
| 8 . . . . | Axial gearbox velocity . . . . . | NAp |
| 9 . . . . | Proximity probe, dc coupled, radial gearbox . . . | NAp |
| 10 . . . | Proximity probe, dc coupled, radial generator . . | NAp |
| 11 . . . | Proximity probe, dc coupled, axial gearbox . . . | NAp |
| 12 . . . | Proximity probe, ac coupled, radial gearbox . . . | NAp |
| 13 . . . | Proximity probe, ac coupled, radial generator . . | NAp |
| 14 . . . | Proximity probe, ac coupled, axial gearbox . . . | NAp |
| 15 . . . | Starter volts . . . . . | NAp |
| 16 . . . | Starter amperes . . . . . | NAp |
| 17 . . . | Starter kilowatts . . . . . | NAp |
| 18 . . . | Type K thermocouple . . . . . | NAp |
| 19 . . . | Motor winding thermocouple . . . . . | NAp |

NAp Not applicable.

## Results

With the 600 A current limit setting, the flywheel spun up to 3,300 rpm and would not advance in speed. Testing was curtailed until the next day, and the current limit on the starter was raised to 700 A. The flywheel was able to reach 6,000 rpm before a stall condition developed. With the current limit set between 850 and 900 A, the flywheel

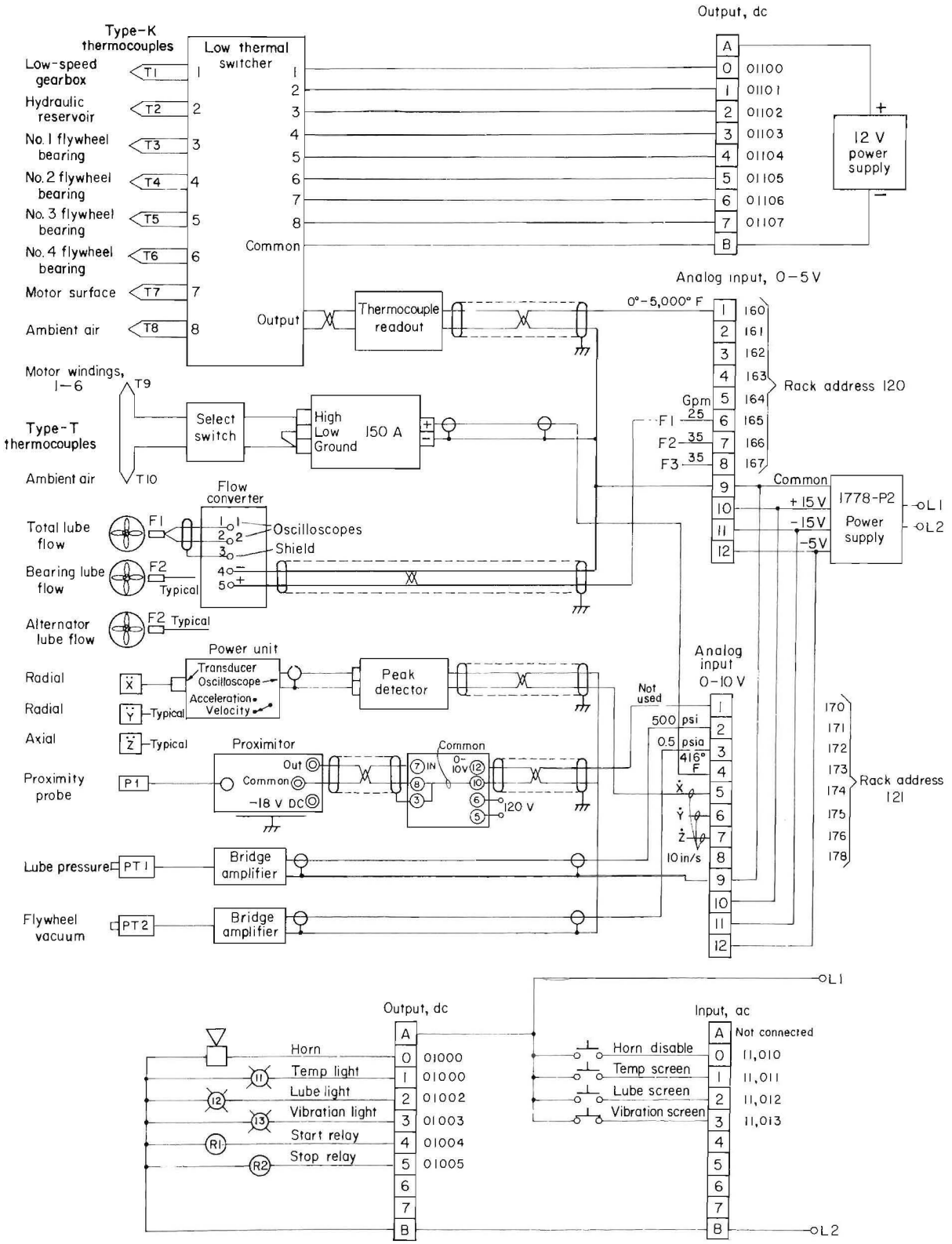


**Figure E-1.—Wiring schematic.**

Table E-3.—Temperature parameters as of 16 May 1986

| Time, p.m. | Flywheel speed, rpm | Temperature, °F | | | | | | | | |
|---|---|---|---|---|---|---|---|---|---|---|
| | | Bearing | | | | Flywheel | | Transmission fluid | Charge motor surface | Motor windings |
| | | 1 | 2 | 3 | 4 | Internal | Surface | | | |
| 1:43 . . | 16,080 | 173 | 160 | 139 | 215 | 99 | 90 | 116 | 148 | 380 |
| 1:55 . . | 12,900 | 174 | 167 | 157 | 230 | 102 | 93 | 135 | 172 | NM |
| 2:00 . . | 11,160 | 171 | 167 | 160 | 219 | 105 | 96 | 143 | 177 | NM |
| 2:19 . . | 15,720 | 200 | 188 | 178 | 257 | 111 | 101 | 149 | 182 | NM |
| 2:33 . . | 11,400 | 185 | 180 | 174 | 242 | 118 | 107 | 154 | 186 | NM |
| 2:51 . . | 6,000 | 155 | 150 | 152 | 180 | 123 | 110 | 140 | 174 | NM |

NM Not measured.

was successfully powered up to 16,700 rpm. This amperage is required to overcome system torque requirements as related to the charge motor torque curve.

Figure E-2 shows the charge-discharge time for the spin up test. A total of 5 min 1 s was required to charge the flywheel to 16,700 rpm from a dead stop. The charging time between 8,400 and 16,700 rpm, which is the operating speed range of the generator, averages 1 min 36 s. Total coast down time from 16,700 to 0 rpm was 1 h 29 min 35 s.

Various temperature measurements were obtained while operating the flywheel package. Table E-2 tabulates the temperature limits on various components. The only temperature out of limits was bearing 4, which is the bearing on the generator side of the flywheel package. Initial temperature limit for the bearing was set at 250° F. The manufacturer was contacted about the hot bearing and responded that the bearing could operate at 300° F without damage. Table E-3 shows bearing 4 temperature increasing during speed increases and decreasing as the flywheel coasts down. This trend suggests the bearing will operate satisfactorily without damage.

Flywheel system performance characteristics were evaluated from the FM tape recorded data and from the data processing system. Hydraulic system characteristics were evaluated by plotting flywheel speed versus system flows. Figure E-3 shows typical system flows with flywheel speed. The 10 gpm limit for total system flow was achieved at 10,000 rpm of the flywheel. The 3 gpm minimum for bearing flow was achieved at 3,000 rpm. The 1 gpm minimum for alternator flow was achieved at 2,000 rpm. Since the operational range of the flywheel will be 8,500 to 16,700 rpm, the flows are all within acceptable limits. Figure E-4 plots system pressure versus flywheel speed. Normal system pressure operating range limits are reached at 4,000 rpm and are well within the duty cycle range of the flywheel package.

The charge motor-starter system was characterized by plotting volts, amps, and kilowatts versus flywheel speed. Figure E-5 shows a typical test plot. Figure E-6 is the charge motor kilowatt parameter integrated to obtain the overall input energy relative to flywheel speed. This plot shows that the flywheel system requires 19 kW·h of energy to reach 16,700 rpm from 0 rpm. The amount of energy stored in the flywheel should equal some percentage of these values after all system losses are determined when the generator is installed in the flywheel package.

Figure E-7 is a plot of the charge motor winding temperature versus spin up time to 16,700 rpm. The

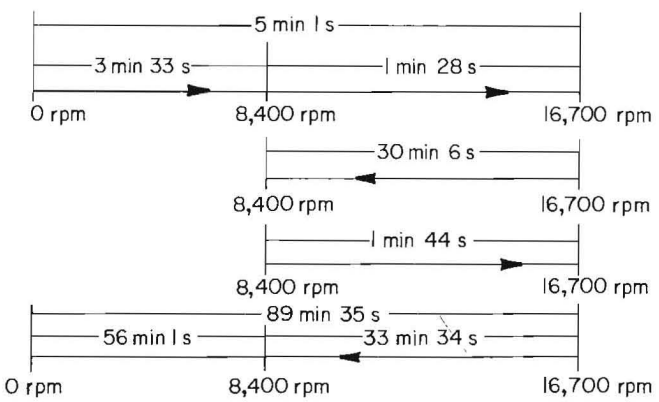


Figure E-2.—Charge-discharge time.

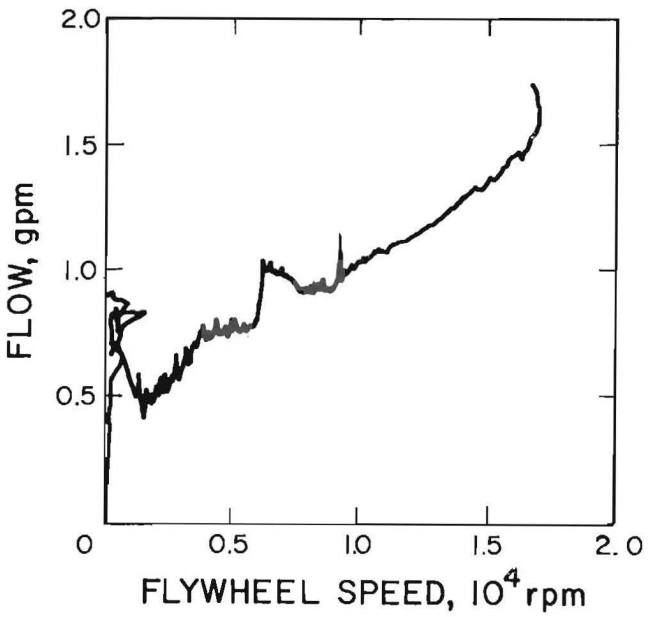


Figure E-3.—System flow versus flywheel speed.

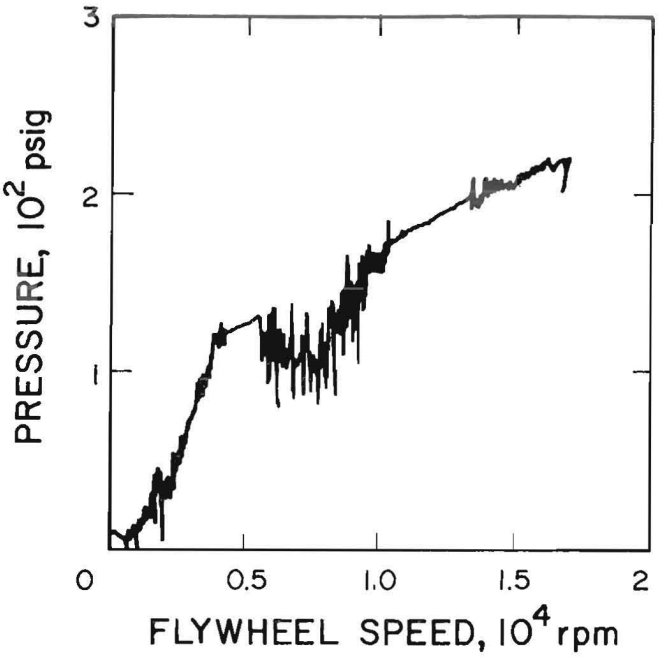


Figure E-4.—System pressure versus flywheel speed.

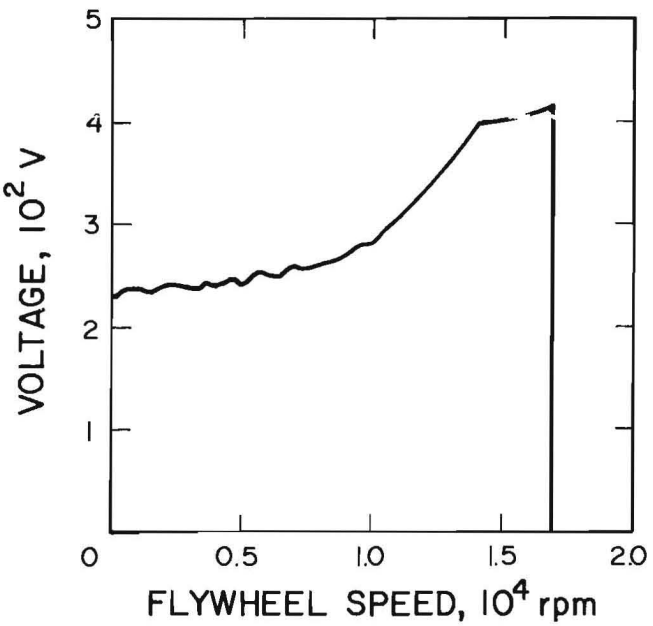


Figure E-5.—Motor-starter voltage versus speed.

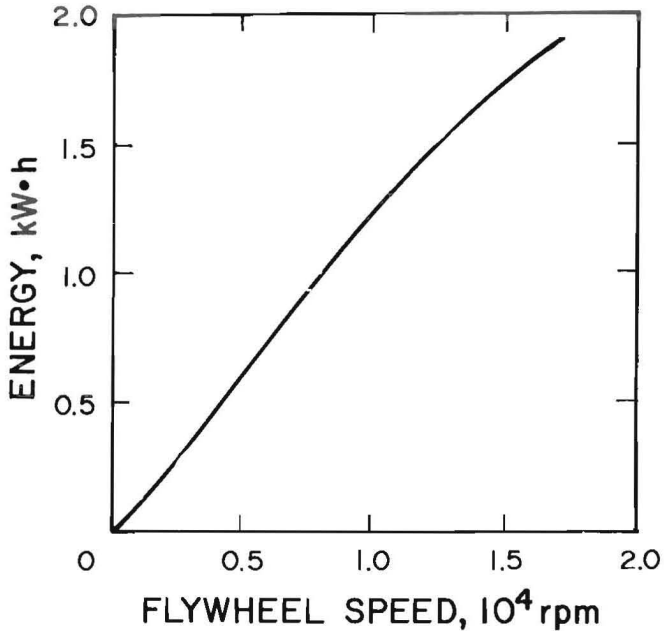


Figure E-6.—Motor-starter input energy versus speed.

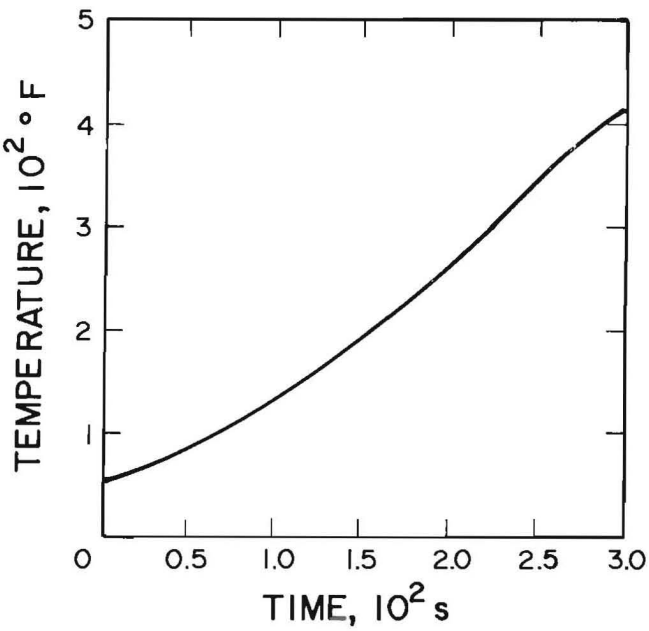


Figure E-7.—Charge motor temperatures.

motor manufacturer recommends that the motor winding temperature should not exceed 425° F. The figure shows that the motor winding temperature is not exceeded, but is very close to the 425° F limit at 410° F. This near limit temperature in the charge motor could be a problem with regard to recharge cycle. A cool down period is required on the motor prior to recharging.

Accelerometers were used to monitor vibration while the flywheel was operated. The accelerometer signal was integrated via an analog integrator supplied by the accelerometer manufacturer to obtain velocity. A spectrum analyzer, in conjunction with a desk-top computer, was used to analyze the velocity data recorded on FM tape. This data can be used to interpret the severity of vibration and rotor vibration characteristics (i.e., unbalance and shaft critical speeds). Figure E-8 is a peak hold spectrum plot of vibration measured at the generator side of the flywheel housing in the radial direction. Vibration due to shaft unbalance tracks directly with running speed and at

critical shaft speeds, the vibration is amplified due to dynamic instabilities. This figure shows there are probably two shaft criticals in the operating speed range of the flywheel. The first critical occurs at 4,800 rpm (80 Hz), and the second critical occurs at 10,680 rpm (128 Hz). Figure E-9 is a cascade plot of the same data depicted in figure E-8. Vibration frequencies that track with running speed or some ratio of running speed form diagonals on the plot.

Frequencies that do not track with speed are structural resonances. Although a shaft critical does exist within the normal operational range of the flywheel [8,500 (142 Hz) to 16,700 rpm (278 Hz)], a fluid damper has been designed into the bearing system to dampen this vibration, and the vibration levels measured are within acceptable limits.

While the flywheel system was operating, a sound level meter was used to measure the sound at a 3-ft distance from the flywheel compartment. A level of 100 dB was measured when the flywheel was at 16,700 rpm. Flywheel compartment covers were not installed during the test. These covers will reduce or have the potential of increasing the noise level.

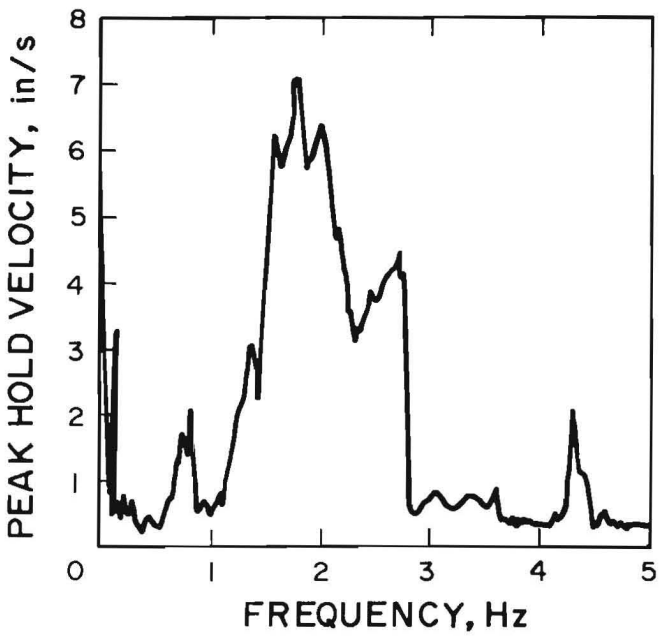


Figure E-8.—Peak hold vibration spectrum.

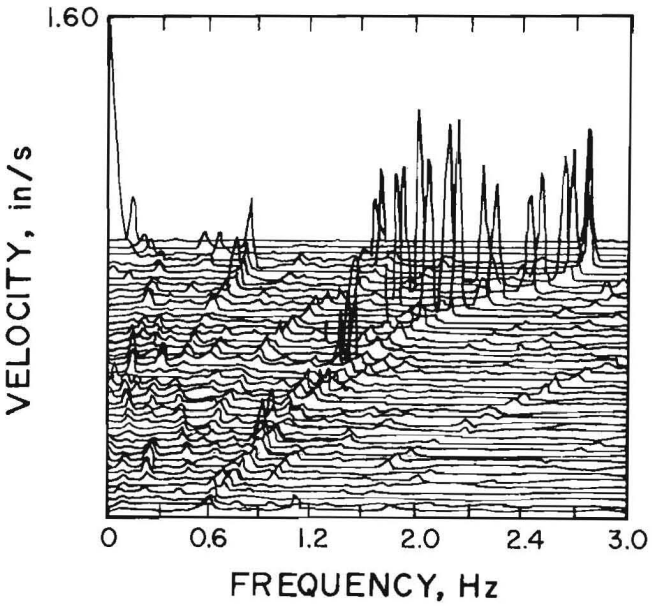


Figure E-9.—Vibration cascade plot.

# APPENDIX F.—FLYWHEEL SPIN UP WITH GENERATOR AND LOAD RESISTOR BANK TESTS

## Setup and Instrumentation

These tests were designed to verify the mechanical and electrical operation of the generator. The flywheel with generator would be spun up to full speed and known resistive loads were engaged to the generator electrical output.

This testing required the design and installation of a resistive load grid on the shuttle car. This grid allowed for various resistive loads to be applied to the output of the generator. The load bank allowed for selective engagement of 5-, 25-, and 45-kW electrical loads. These resistors were of significant size and required fixturing to allow installation within the shuttle car conveyor. The output of the generator was instrumented for dc voltage and current measurement. These transducers constituted the final addition to the overall instrumentation package developed throughout the test program. The generator volts and amperes were output to a strip chart and FM tape recorder. A FM tape log sheet for the parameters was recorded while testing.

## Procedure

The generator was lube tested using the fixturing described in appendix C prior to installation on the shuttle car. With the flywheel package installed on the shuttle car and the generator interfaced to the load bank resistors, the flywheel and generator were brought up to full speed of 16,700 rpm. The 5-kW load bank was engaged and the generator activated. The flywheel and generator coasted down to approximately 8,500 rpm under the 5-kW load. The charge motor was then activated to charge the flywheel system back up to 16,700 rpm. The 25-kW load bank was then engaged, and the flywheel coasted down to 8,500 rpm. The spin up sequence was repeated and the 45-kW load engaged while the flywheel coasted down in speed. Generator volts and amperes along with other system parameters were recorded on FM tape throughout the course of testing.

## Results

All mechanical and electrical systems functioned properly during flywheel charging and with generator load test operation. After successfully completing the load test sequence, the data recorded on FM tape was analyzed. Figures F-1 through F-5 are plots of generator voltage, ampere, wattage, speed, and energy with 45 kW of the resistive load applied to the generator output. These plots provide valuable information about the flywheel systems capability for powering the shuttle car through a mine haulage duty cycle.

The power delivered by the generator was obtained via computer multiplication of the generator voltage and ampere data recorded on FM tape. The energy plot was derived from integrating the power plot. The generator speed plots were generated by using a period to voltage converter on the recorded proximity probe sensor's data. The proximity probes were installed in the flywheel housing and generated a one pulse per revolution signal as the flywheel rotor turned.

The voltage and ampere plots show that the generator package was able to supply steady-state voltages and amperes for each of the resistive loads applied to the generator output. The data also show that the cycle time decreased as the load increased. This cycle time is based on the speed of the flywheel. Operational requirements

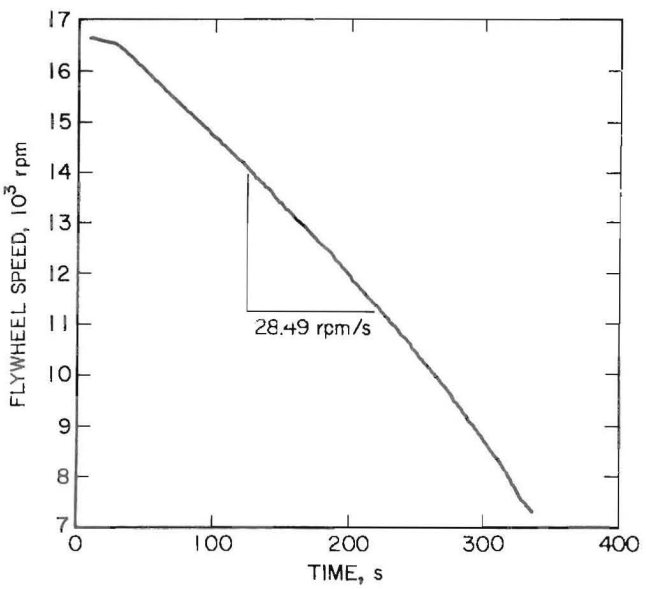


Figure F-1.—Flywheel speed versus time 45 kW load.

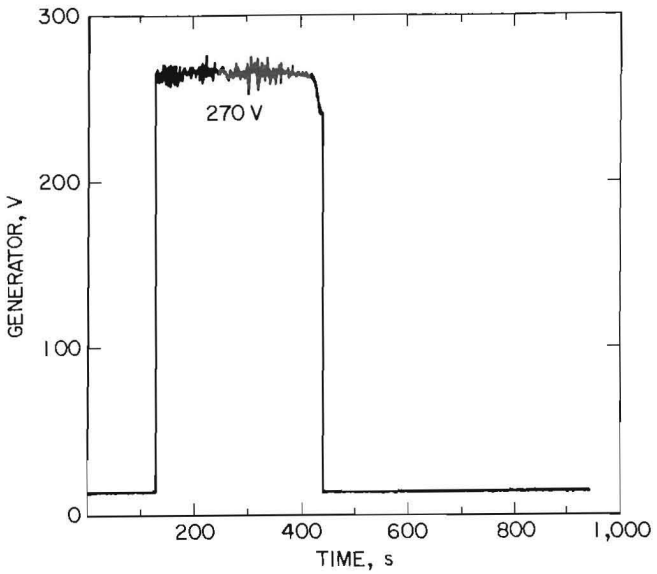


Figure F-2.—Generator voltage 45 kW load.

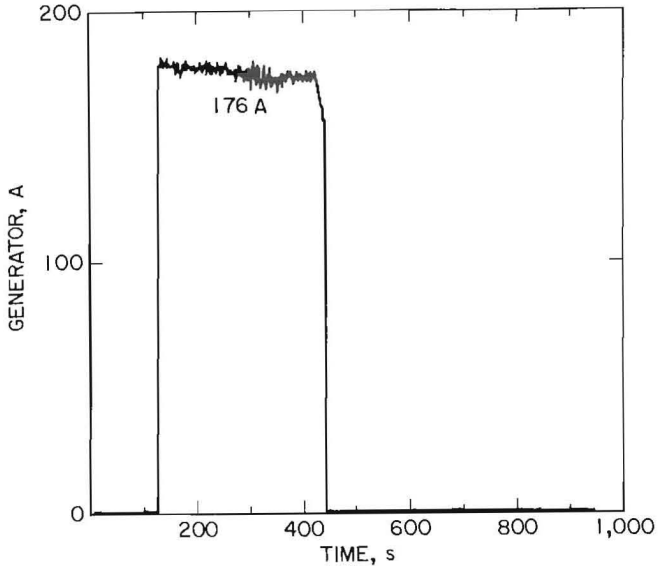


Figure F-3.—Generator ampere 45 kW load.

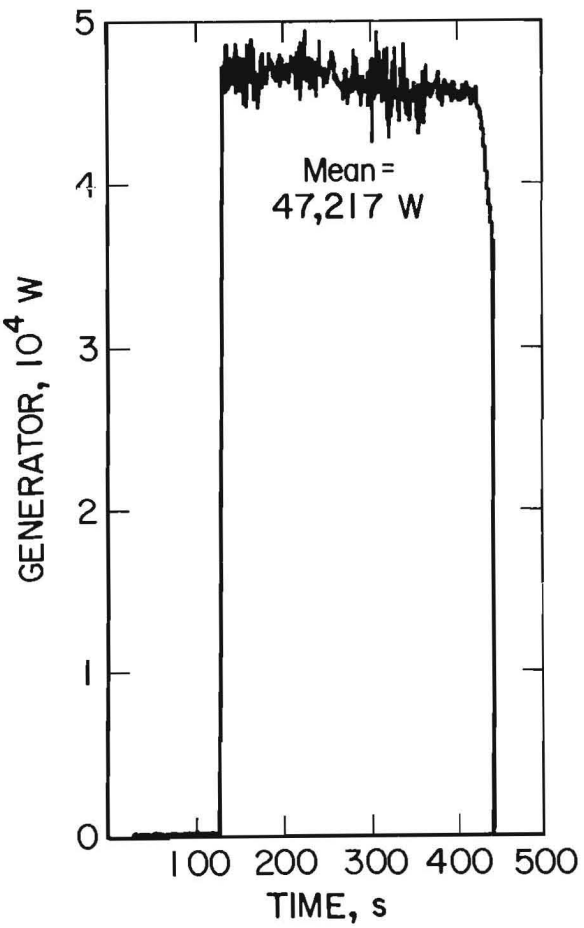


Figure F-4.—Generator wattage 45 kW load.

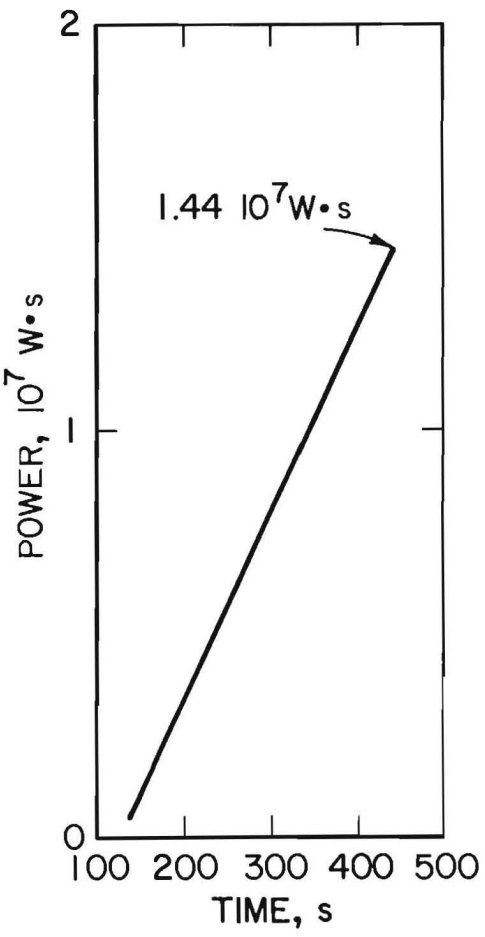


Figure F-5.—Energy delivery 45 kW load.

call for a speed cycle range between 8,500 and 16,700 rpm for the mine haulage duty cycle.

The flywheel speed plots for the various loads show a linear speed decrease with time. Table F-1 tabulates the slope for the generator revolution per minute measured for each of the load conditions tested. A plot of the slopes versus load shows a linear relationship between the two parameters. Figure F-6 shows a linear curve fit of these parameters with the following equation:

$$y = 4.39 + 0.535x$$

where $y$ = generator speed-time slope

and $x$ = generator load, kW.

**Table F-1.—Power-slope tabulation**

(Flywheel designed to deliver 4.5 kW·h usable energy; total usable energy of 6.22 kW·h)

| Power, kW | Slope rpm, s | Delta time, 16,700 to 6,700 rpm, s | Run time, min | Energy, kW·h |
|---|---|---|---|---|
| 0 ..... | -3.30 | 3,030 | 50.5 | 0 |
| 5 ..... | -8.43 | 1,186 | 19.77 | 1.65 |
| 25 ..... | -17.49 | 572 | 9.53 | 3.97 |
| 45 ..... | -28.49 | 351 | 5.85 | 4.38 |

This equation considers power losses due to mechanical inefficiencies and aerodynamic drag on the flywheel power system. Generator speed is the major factor with regard to the mine haulage duty cycle. The generator will stop functioning when it gets below 6,500 rpm.

The equation determined for generator speed versus kilowatt load can be applied to the duty cycle to evaluate if the cycle can be accomplished. Table F-2 tabulates the loads and run times for each portion of the proposed cycle. The delta revolution per minute column shows the generator change in speed due to that portion of the duty cycle. A total change of 10,000 rpm is indicated for the proposed duty cycle. This delta revolution per minute change places the generator speed at 6,700 rpm, which is the borderline for recharge sequence to begin. The generator will stop functioning below 6,000 rpm. This duty cycle does have some dead time built into it so that there is some margin for error.

**Table F-2.—Mission duty cycle tabulation**

(9,998.7 delta rpm total)

| Parasitics | Load, kW | Slope rpm, s | Time, s | Delta, rpm |
|---|---|---|---|---|
| Losses .. | 11 | 10.28 | 327 | 3,362 |
| Tram ... | 33 | 22.0 | 88.6 | 1,953 |
| Load ... | 8.4 | 8.87 | 55.6 | 493 |
| Haul .... | 56 | 34.35 | 122 | 4,190 |

Figure F-7 is a revised duty cycle. Substituting values into the speed-load equation again predicts generator revolution per minute for the proposed duty cycle. The final speed of 8,926 rpm was determined for this duty cycle. However, there is no wait time built into this cycle.

These duty cycles are theoretical and final evaluation would have to be determined from actual testing with the machine operating under flywheel power. Interface of the generator to the shuttle car power control circuitry was accomplished and testing completed.

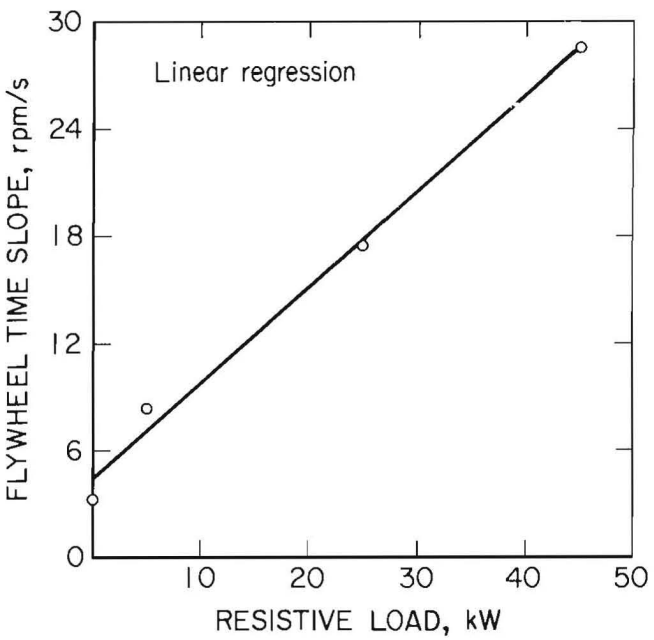


**Figure F-6.—Speed versus load.**

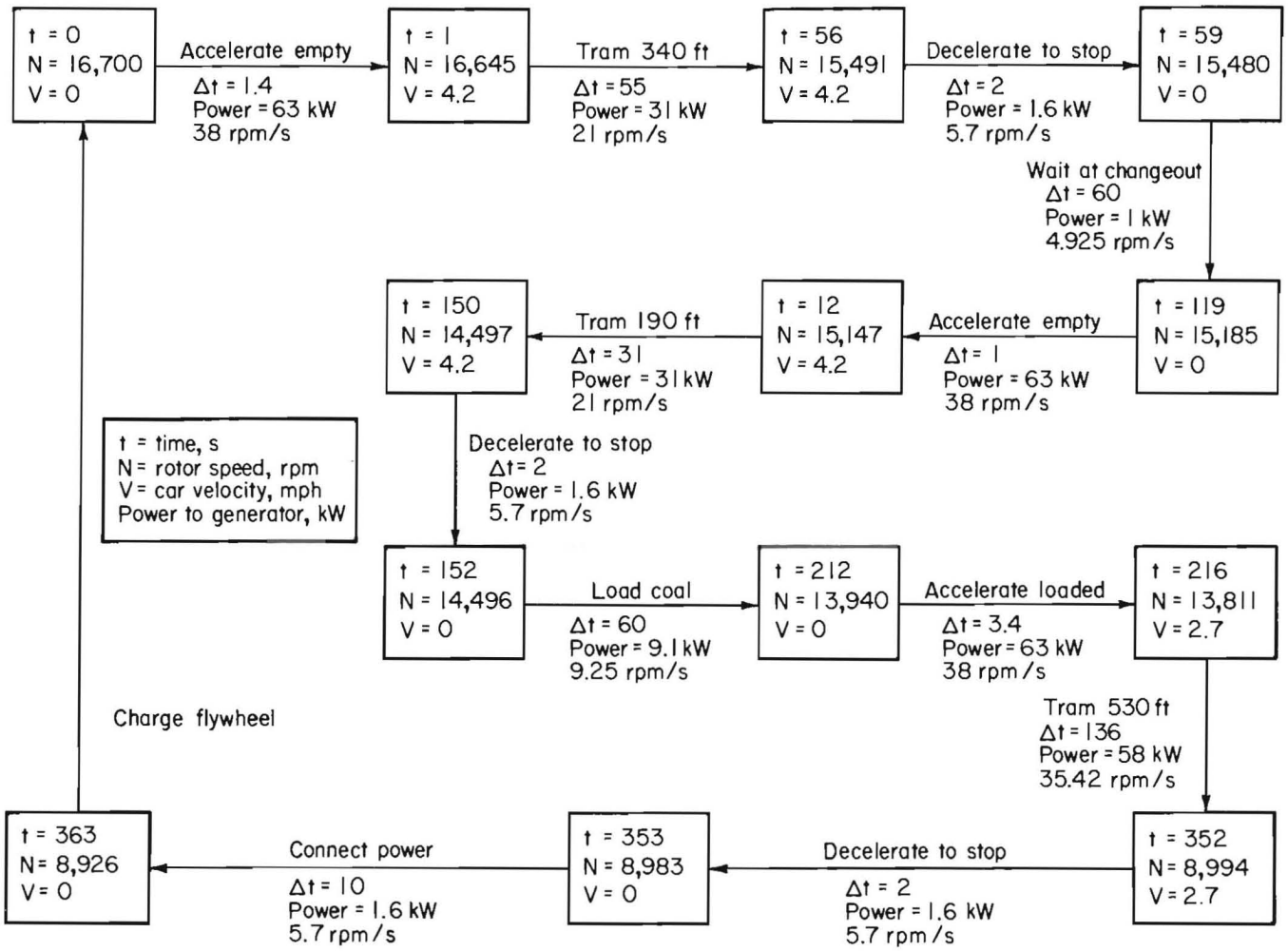


**Figure F-7.—Mission duty cycle power requirements.**

# APPENDIX G.—FLYWHEEL POWER PACKAGE INTERFACED TO SHUTTLE CAR POWER CONTROL CIRCUITRY

## Test Setup and Instrumentation

The FPSC was trammed over a given course to evaluate the flywheel power package with regard to duty cycle operation. The following is a description of the interface configuration of the generator to the shuttle car power circuitry.

1. A 5-kW resistive load bank was placed between the generator output and shuttle car input. This resistive bank would provide a continuous static load for generator transient protection.
2. The capacitors and inductors associated with the shuttle car power control system were eliminated.
3. The SCR traction motor speed control circuitry was replaced with a simplified contractor control circuitry from another shuttle car.
4. Resistors were added in series to the traction motor power inputs to limit current during transient intervals to 125 A.
5. The shuttle car monitoring system at the operator's station was disconnected.

## Procedure

The shuttle car interface circuitry was tested via power obtained from the power center before final connection to the generator output circuit. A gasoline-powered generator was used to supply power to the instrumentation now mounted within the shuttle car conveyor. The shuttle car was fully instrumented and could now operate untethered. The flywheel was brought up to full speed using the solid-state starter charging system. The power center for the solid-state starter was shut off and the power cable between the starter and shuttle car charge motor disconnected. The generator was then activated along with the shuttle car pump circuitry. The operator then engaged the tram circuitry and trammed a predetermined course. The flywheel speed was continuously monitored while tramming, and when flywheel speed reached 12,000 rpm, the operator reversed directions and trammed back to the solid-state starter charging station. The flywheel was then allowed to come to a complete stop. The same instrumentation system used for the resistive load test was used for this test sequence.

## Results

All mechanical and electrical systems functioned properly. The shuttle car trammed 634 ft in 6 min 23 s for an average tram speed of 1.13 mph. Figure G-1 shows that the time required to charge the flywheel from 0 to 16,700 rpm was 5 min 31 s. During the charge sequence it was often noted that the charge motor windings came close to and often exceeded the 425° F winding temperature operational limit. Figure G-2 is a plot of charge motor winding temperature versus time during the flywheel charge sequence. A period of time would be required before the flywheel could be recharged for the duty cycle to resume. Figure G-3 is a plot of charge motor temperature against time after the initial charge sequence. The following equation expresses the cooling rate depicted by figure G-4 with an ambient temperature of 72° F:

$$y(x) = a + b * x$$

where $a = 421°$ F,

$b = -0.333°$ F/s,

$x$ = time, s,

and $y$ = motor winding temperature, °F.

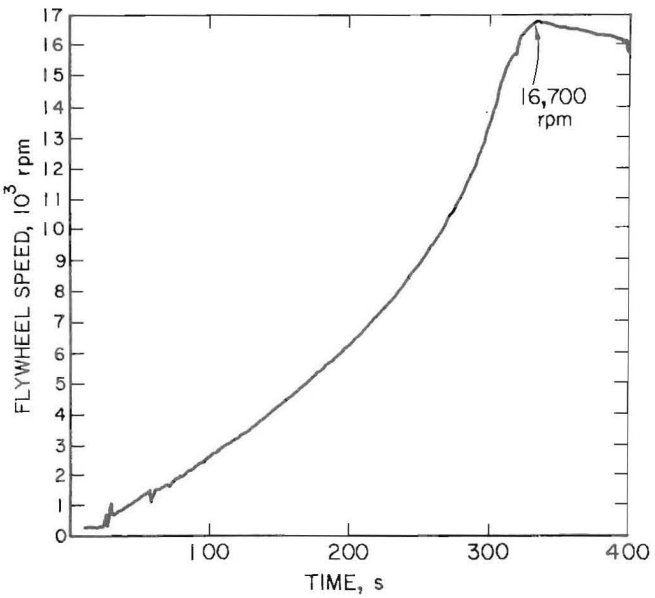


**Figure G-1.—Flywheel speed versus charge time.**

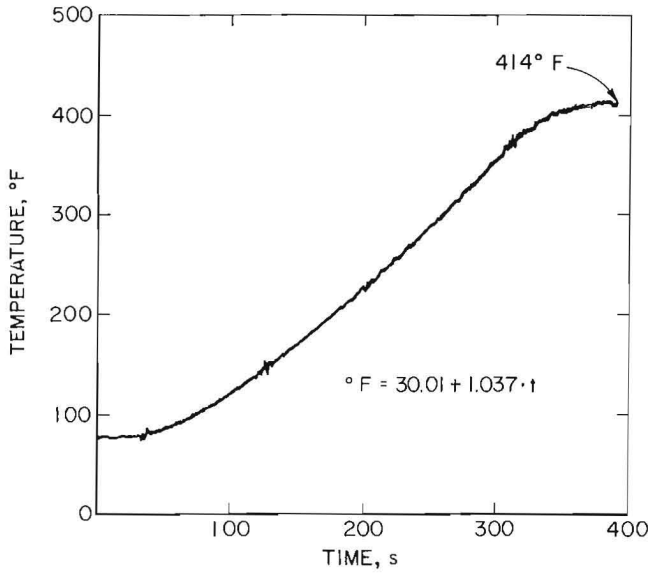


**Figure G-2.—Winding temperature.**

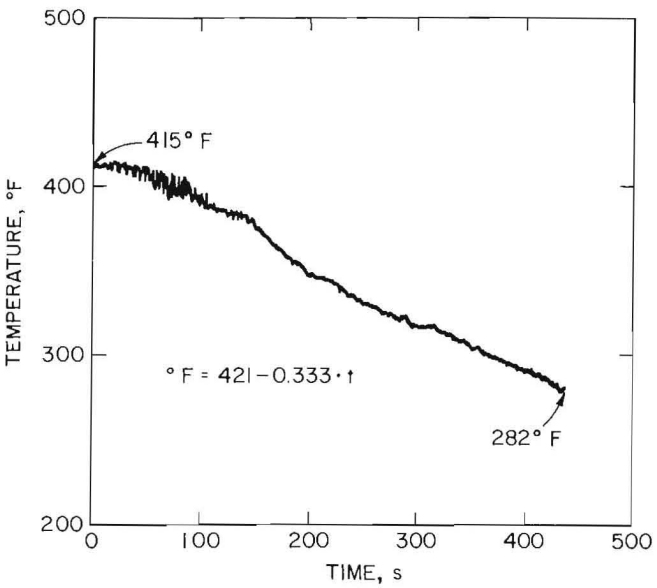


**Figure G-3.—Winding cool down.**

Figure G-3 shows that during the charging sequence the charge motor temperature was approximately 220° F when the rotor was at 6,500 rpm. This temperature would represent the minimum temperature the motor would have to reach before recharging would occur. Using this equation, it will take 10 min 26 s before a duty cycle recharge can occur without overheating the charge motor windings.

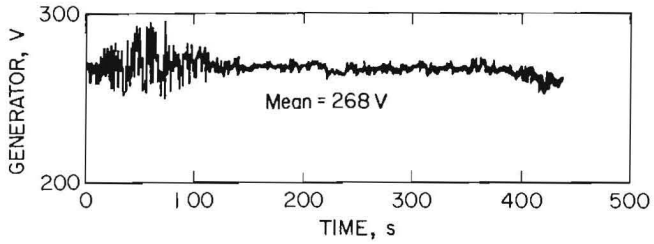


**Figure G-4.—Generator voltage while tramming.**

This cycle time will be reduced with the anticipated lower ambient temperature associated with coal mines.

Figure G-4 is a plot of the generator voltage during the tram testing. The mean value for the volts generated is 268 V. Figure G-5 is a plot of flywheel-generator speed versus time for the tram test. The curve has a linear slope. The hump in the middle shows a change in slope that can be associated with an idle condition while the operator reversed tram directions when the speed was at approximately 12,000 rpm. The final speed reached when the machine returned to the charging station was 6,642 rpm. The generator was still functioning at this speed. Figure G-6 plots generator current versus time for the tram test.

The mean amperes was 93.23 A, which is well within the 167 A maximum range of the generator.

Figure G-7 is a plot of the power output of the generator while tramming. The mean value for this power was 25 kW. Figure G-8 is a plot of the overall energy delivered during the 6 min 23 s tram test. Conversion of the watt-seconds to kilowatt-hours results in a total of 3.06 kW • h of energy delivered to the shuttle car by the flywheel power package. This value fits well into the design requirements specified at 4.5 kW • h of usable energy for the recycle speed range. Figure G-9 is a time histogram with the 5-kW resistive load removed mathematically since the resistor bank was not doing any useful work.

The speed control used for this test only allowed for approximately 1-mph tram speed. The theoretical duty cycles presented in appendix F calls for tram speeds of 4 mph while tramming empty and 2.7 mph when loaded. These higher tram speeds reduce the time for which energy is expended for tramming. The time required to complete the tram test was longer than the proposed duty cycle which involved loading, unloading, and a wait time.

This test has proven that the flywheel energy system can function and operate the shuttle car. Gyroscopic effects were insignificant with regard to vehicle steerability. The

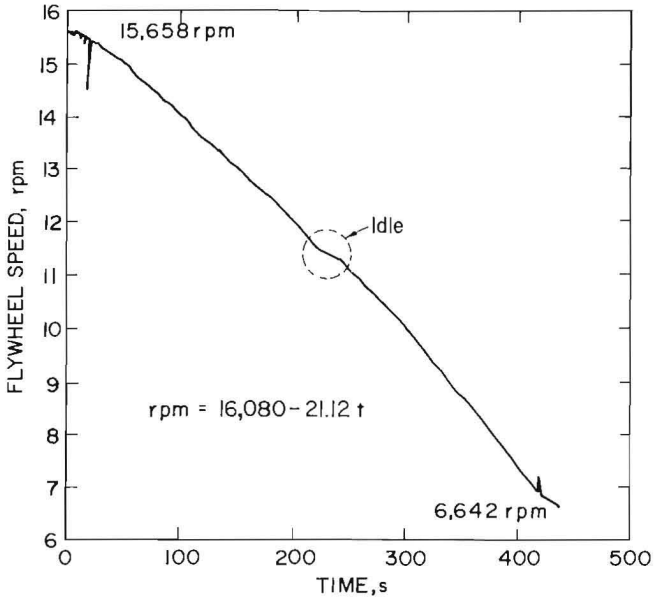


Figure G-5.—Flywheel speed while tramming.

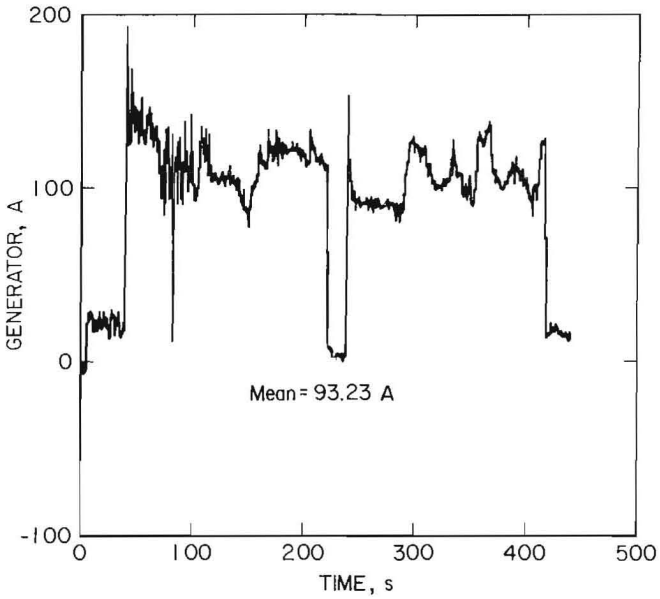


Figure G-6.—Generator ampere while tramming.

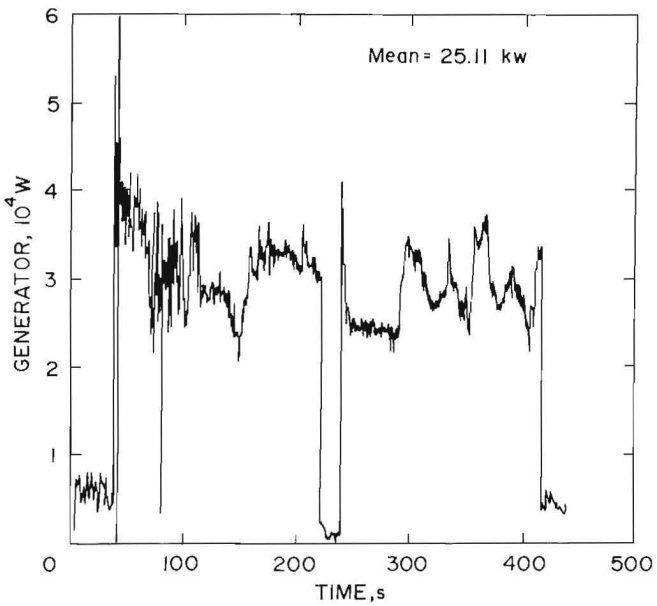


Figure G-7.—Generator wattage while tramming.

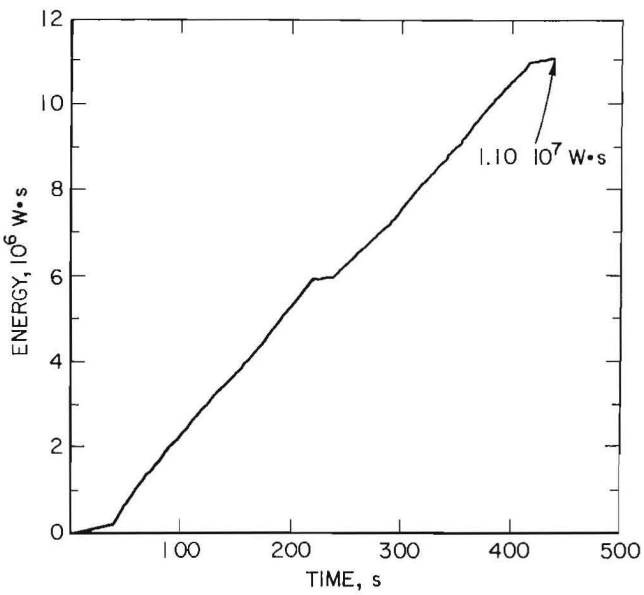


Figure G-8.—Generator energy while tramming.

major drawback now involves the speed control and interface to the shuttle car from the generator. The current system would not meet duty cycle requirements. The generator to shuttle car power circuitry needed to be optimized to obtain higher tram speeds.

Final optimization of the shuttle car tram circuitry took the form of an interface arrangement between the solid-state chopper drive and the flywheel power package. This was the original speed control for the tram. The solid-state drive provided the most efficient use of the available

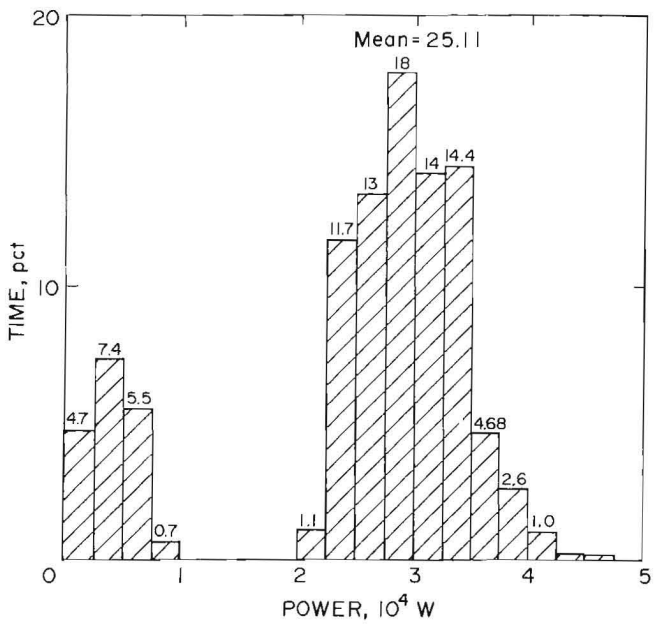


**Figure G-9.—Power while tramming 5 kW load.**

stored energy in addition to the precise tram power control that will achieve the desired mission duty cycle.

The FPSC was retrofitted with a solid-state control circuit and interface circuit between the control circuit and the GCU. These system changes increased the efficiency by 33 pct. In addition, the solid-state circuitry allowed variable control of the tram circuit, which replaced the on-off type operation that was previously on the machine. Results from the surface testing indicate that the solid-state circuitry will increase the tram rate by 1 to 4 mph, thereby satisfying the original design specifications. The final surface test was the completion of a typical mission duty cycle with a typical load of coal. The shuttle car was able to complete the duty cycle at an average speed of 3.5 mph, thereby making it competitive with conventional shuttle cars with trailing cables.